Review

A Review on Electrochemical Advanced Oxidation Treatment of Dairy Wastewater

Ashish Kumar Das [1] and Lide Chen [2,*]

1   Environmental Science, College of Natural Resources, University of Idaho, Moscow, ID 83844, USA; das7853@vandals.uidaho.edu
2   Department of Soil and Water Systems, Twin Falls Research and Extension Center, University of Idaho, 315 Falls Avenue East, Twin Falls, ID 83301, USA
*   Correspondence: lchen@uidaho.edu; Tel.: +1-208-736-3615

Abstract: Dairy wastewater (DW) contains a high concentration of organic and inorganic pollutants. In recent years, extensive research has been conducted to develop more efficient techniques for the treatment of DW. Electrochemical advanced oxidation processes (EAOPs) have gained significant attention among the various treatment approaches. EAOPs rely on electrochemical generation of hydroxyl radicals ($\bullet OH$) which are considered highly potent oxidizing compounds for the degradation of pollutants in DW. In this paper, we provide an overview of the treatment of DW using various EAOPs, including anodic oxidation (AO), electro-Fenton (EF), photo electro-Fenton (PEF), and solar photo electro-Fenton (SPEF) processes, both individually and in combination with other techniques. Additionally, we discuss the reactor design and operating parameters employed in EAOPs. The variation in degradation efficiency is due to different oxidizing agents produced in specific approaches and their pollutant degradation abilities. In AO process, $\bullet OH$ radicals generated on electrode surfaces are influenced by electrode material and current density, while EF procedures use Fe^{2+} to create oxidizing agents both on electrodes and in the DW solution, with degradation mechanisms being affected by Fe^{2+}, pH, and current density; additionally, PEF and SPEF approaches enhance oxidizing component production and pollutant degradation using ultraviolet (UV) light. Integration of EAOPs with other biological processes can enhance the pollutant removal efficiency of the treatment system. There is a scope of further research to exhibit the effectiveness of EAOPs for DW treatment in large scale implementation.

Keywords: dairy wastewater; electrochemical advanced oxidation process; anodic oxidation; electro-Fenton; photo electro-Fenton; solar photo electro-Fenton

1. Introduction

The dairy sector is booming globally due to the increasing demand for milk and dairy commodities [1]. Global milk production climbed to around 950 million tons in 2021 [2]. Dairy operation practices often require a huge quantity of water, which induces dairy wastewater (DW). Our study shows that approximately 2–2.5 L of DW are generated for each liter of milk production [3]. This DW may contain significant amounts of organic and inorganic contaminants such as chemical oxygen demand (28,000–34,000 mg/L), total organic carbon (2000–3000 mg/L), biochemical oxygen demand (25,000–30,000 mg/L), total phosphorous (900–1500 mg/L), ortho-phosphate (700–1000 mg/L), ammonia–nitrogen (1500–2000 mg/L), total nitrogen (25,000–3000 mg/L), total solid (3–7%), and total suspended solid (2–5%), and the pH of DW may varies from 7.5 to 8.5 [4,5]. These contaminants can hamper environmental sustainability if they are mixed into the ecosystem. The current DW management systems are not efficient in removing all types of contaminants. Consequently, discharging partial treated DW can create adverse environmental impacts, such as eutrophication and oxygen depletion in surface and subsurface water sources. Therefore,

appropriate DW treatment practice is essential for the betterment of our environment [6,7]. The adoption of approaches like zero-liquid discharge and the utilization of recovered resources from DW would significantly contribute to mitigating the environmental pollution [8–16].

The treatment of DW entails the utilization of both physicochemical and biological treatment methods [17,18]. Physicochemical techniques encompass the usage of membrane technologies [19], coagulation–flocculation [20], and similar approaches, while biological processes involve aerobic and anaerobic methods like the activated sludge process [13,21,22], lagoons [23], sequencing batch reactors (SBRs) [24,25], and up-flow anaerobic sludge blankets (UASBs) [26]. Nevertheless, the capacity to remove soluble organic pollutants using physicochemical methods is restricted, and the expensive nature of reagents has prompted a notable shift towards biological methods to remove pollutants from DW. However, these traditional processes are accompanied by various disadvantages, such as substantial capital and energy demands, as well as significant sludge generation. The substantial energy requirements of the treatment systems have further emphasized the necessity for alternative treatment approaches, which are economically viable and entail minimal energy consumption [27–29].

Over the period of three decades, extensive research has been carried out to enhance the effectiveness of technologies aimed at fully eliminating contaminants [14]. In such circumstances, advanced oxidation processes (AOPs) have become a pivotal area of attention. AOPs operate by producing extremely reactive hydroxyl radicals ($\bullet$OH) on-site, which then engage with both organic and inorganic contaminants, enabling the breakdown of even the most persistent substances [30–33]. These radicals are considered the most potential oxidants with a notable oxidation/reduction potential of 2.80 volt (V) per standard hydrogen electrode (SHE) [34,35]. Furthermore, $\bullet$OH radicals have a brief lifespan, estimated to be mere nanoseconds in water, enabling their natural elimination from the treatment system [36]. The most commonly employed AOPs include combinations of hydrogen peroxide (H_2O_2) with ultraviolet (UV), such as hydrogen peroxide coupled with UV-C (H_2O_2/UV-C), ozone-based approaches (O_3/H_2O_2, O_3/UV-C, and O_3/H_2O_2/UV-C), titanium dioxide-based methods (TiO_2/H_2O_2/UV, TiO_2/UV), as well as Fenton-reaction-based approaches, such as Fenton process (Fe^{2+}/H_2O_2) and photo-assisted Fenton process (Fe^{2+}/H_2O_2/UV), etc. [37,38].

In recent times, electrochemical advanced oxidation processes (EAOPs) have gained attention due to having high pollutant-removal efficiency in DW treatment [37–41]. Anodic oxidation (AO) is a basic, straightforward, and widely used form of EAOP, where organic compounds can undergo direct oxidation on anode surfaces through electron transfers. Alternatively, they can undergo indirect oxidation through $\bullet$OH radicals, which are weakly adsorbed on the anode surface, and/or active chlorine (ClO^-), ozone (O_3), persulfates ($S_2O_8^{2-}$), and hydrogen peroxide (H_2O_2), like other radicals present in the bulk solution [42,43]. When the cathodic electro-generation of H_2O_2 is incorporated into AO, it gives rise to a process known as H_2O_2 electro-generated anodic oxidation (AO-H_2O_2) [44]. The frequent and extensively researched electro-Fenton (EF) approach is established through the electro-generation of H_2O_2 radicals in the presence of ferrous ion (Fe^{2+}) in the wastewater solution, resulting in the production of additional $\bullet$OH compounds through a Fenton-like reaction [45]. Furthermore, research conducted by Brillas et al. [41] combined ultraviolet radiation with a Fenton reaction either artificially or naturally. The artificial procedure is referred to as photo electro-Fenton (PEF), while the natural approach is recognized as solar photo electro-Fenton (SPEF). The SPEF process has the advantage of saving energy consumption, as sunlight is used as major source of UV radiation instead of using artificial light [38,46,47].

Several research projects have been conducted to treat DW by utilizing the electrocoagulation (EC) process where iron (Fe) and/or aluminum (Al) made electrodes have been employed as the anode and cathode, respectively [48–50]. Bazrafshan et al. [51] investigated the impacts of reaction time, applied voltage, and the number of electrodes to treat DW by

using the EC process. They found the chemical oxygen demand (COD), biochemical oxygen demand (BOD$_5$), and total suspended solid (TSS) removal to be 98.84%, 97.95%, and 97.75%, respectively, for 60 V applied voltage at 60 min treatment time. However, the EC process has some problems, including the decaying of electrodes and generating sludge [47]. By overcoming these drawbacks, EAOPs exhibit good pollutant removal performances in regard to synthetic and real wastewater [47,52–59]. Recently, Martínez-Sánchez et al., [60] reviewed EO, EF, and PEF approaches to treating dye-, pharmaceutical-, and pesticide-contaminated wastewater. They reported on different hybrid systems for novel arrangements of different reactors. In their review, Moreira et al. [38] highlighted certain limitations of Fenton-based operations with a lower pH in the wastewater sample and the requirement for an additional treatment step to comply with legal discharge limits by removing the catalyst from the solution. To overcome these drawbacks, a potential solution lies in the development of effective immobilized catalysts. Ganta et al. [14] focused in their review article on the challenges of treating DW and highlighted the potential of microbial electrochemical technologies (METs) as efficient and sustainable solutions. They emphasized the need for further optimization of operational parameters and the development of cost-effective catalysts and membranes to enable the widespread implementation of METs in real-world applications. Ghime and Ghosh [61] highlighted the challenges posed by organic compounds in wastewater and emphasized the potentiality of EAOPs. They overviewed the fundamentals, reaction mechanisms, experimental parameters, and applications of these electrochemical treatment technologies, emphasizing their effectiveness in eliminating organic compounds in aqueous systems. Shokri et al. [62] reviewed the efficiency of EF technology in degrading recalcitrant organic pollutants in waste streams, highlighting it as a promising solution for addressing water-related challenges. They also highlighted the operational capability, eco-friendliness, and pH effectiveness of EF technology, while also discussing the crucial mechanisms, catalyst properties, and operating parameters. The review identifies the major challenges hindering commercialization and proposes research pathways, such as advanced catalyst synthesis, life-cycle assessments, scale-up, reactor design improvements, and hybridization with other treatment technologies, to overcome these challenges and achieve the realistic goal of commercializing EF technology [62].

The objective of this review was to provide an extensive reference for researchers in need of comprehensive details on DW treatment. It focused on the utilization of several EAOPs in terms of AO, EF, PEF, and SPEF, both independently and in conjunction with other technologies. The article discussed various factors that influence the effectiveness of different EAOPs. Additionally, it offered insights into the characteristics of different reactors and electrodes that are suitable for specific EAOPs. To the best of our knowledge, there has been no previous review article that specifically examines the use of EAOPs for treating DW. Thus, there is a gap in the utilization of EAOPs for the management of DW. To address this gap, this review aimed at providing a comprehensive understanding of the various EAOPs-based treatment methods while focusing on the application of EAOPs for treating DW, simultaneously investigating the opportunities for recovering value-added products. Hence, this review intended to be a valuable guide for developing a more efficient DW treatment system based on EAOPs.

2. Fundamentals of Different EAOPs

2.1. Anodic Oxidation Process

The most widely used electrochemical method for the oxidation of contaminants in wastewater is electrochemical oxidation, often known as anodic oxidation (AO). Comninellis [63] presented the mechanism that has been commonly accepted for the oxidation of organic contaminants in aqueous solution (Figure 1). Therefore, the basic AO mechanism can be deduced from Figure 1, where electrodes, especially anodes, can be categorized as active or inactive electrodes, based on the kind of anode material and the nature of active agents exhibiting physicochemical behavior on the surface of an anode.
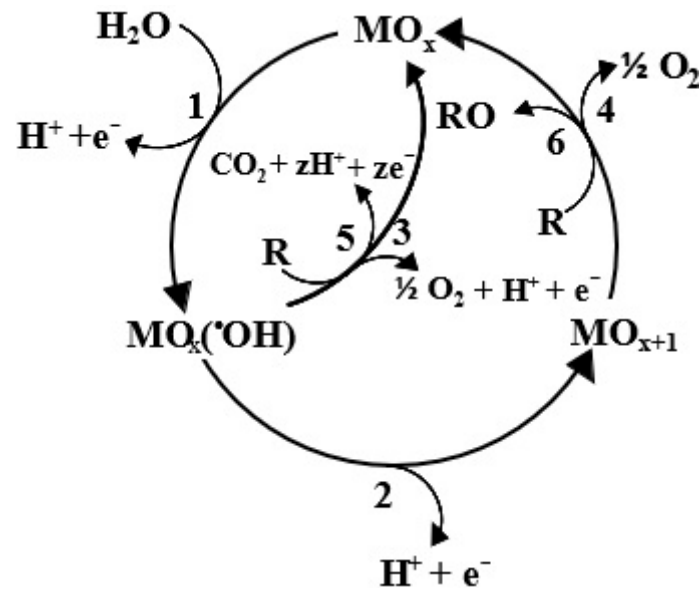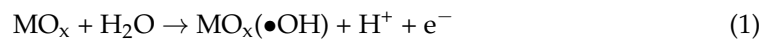
Figure 1. Anodic oxidation mechanism for the degradation of organic pollutants in waste stream (adapted with permission from Ref. [63]. 1994, Comninellis).

As per the expression in Equation (1), active-type anodes (depicted as 1, 2, 4, and 6 in Figure 1) release H_2O to generate •OH radicals, which, initially, adhere to the surface of anodic oxide (MO_x) [63]:

$$MO_x + H_2O \rightarrow MO_x(\bullet OH) + H^+ + e^- \tag{1}$$

To generate the surface site MO_{x+1} for superoxide (Equation (2)), the •OH radical that has been adsorbed proceeds to interact with the MO_x [45].

$$MO_x(\bullet OH) \rightarrow MO_{x+1} + H^+ + e^- \tag{2}$$
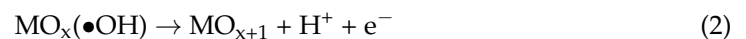
Subsequently, the MO_{x+1} site undergoes selective organic oxidation, as indicated in Equation (3) [63].

$$R + MO_{x+1} \rightarrow MO_x + RO \tag{3}$$

Consequently, active anode only partially oxidizes organic pollutants (R) to (RO) because it can solely engage with the reactive surfaces. This limitation arises from the robust engagement between the electro-generated •OH compounds and the surface of the anode. Equation (4) illustrates that side reactions may also occur at these reactive superoxide anodic sites, leading to spontaneous deactivation. This can lead to efficiency restrictions in the process of organic degradation [38,47].

$$MO_{x+1} \rightarrow 1/2\, O_2 + MO_x \tag{4}$$

Additionally, low O_2 evolution overpotential of active anodes makes them rapidly undergo oxidation to form water. Such electrodes generally comprise metal oxides, denoted as MO_x, capable of creating a surface MO_{x+1} site and distinguished by a reduced potential for O_2 evolution. Examples of active anodes include platinum (Pt), iridium (iv) oxide (IrO_2), and ruthenium (iv) oxide (RuO_2) substrates [46]. As reported by Anglada et al. [64], active anodes exhibit O_2 evolution potentials that are generally below 1.9 V compared to SHE. Therefore, the O_2 evolution reaction is catalyzed in the anodic zone, resulting in the formation of O_2 bubbles on the anode surface. As a result, active anodes are not ideal choices for EO treatments of organic pollutants, as the bubbles formed obstruct the surface of the active anode, hindering the production of •OH radicals [65]. Applying a lower

current density for hindering the O_2 evolution reaction is a suggested remedy for this issue; however, the combined effect results in unfavorably lengthy treatment periods [66].

Contrarily, the contact between •OH radicals and the surface of non-active anodes are modest (1, 5 and 3 in Figure 1), and as a result, their reactions with organic molecules are simple. According to Equation (5), weakly adsorbed •OH compounds on the anode surface have the ability to immediately mineralize pollutants [46].

$$R + MO_x\,(\cdot OH) \rightarrow M + mCO_2 + nH_2O + nH^+ + ne^- \tag{5}$$
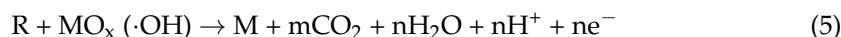
Thus, R undergoes complete oxidation, resulting in the production of CO_2 and H_2O. Similar to active electrodes, unfavorable side effects (Equations (6) and (7)) conflict with the mechanism outlined in Equation (5) [63].

$$MO_x\,(\cdot OH) \rightarrow MO_x + 1/2O_2 + H^+ + e^- \tag{6}$$

$$2M(\cdot OH) \rightarrow 2MO + H_2O_2 \tag{7}$$
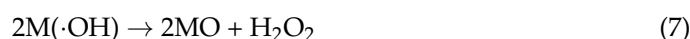
The radicals produced by electrochemistry in non-active anodes are physiosorbed on the surface of the electrode and are only loosely bonded to the anode surface rather than being incorporated within the crystal lattice of the oxide material. The scarcity of available space for hosting oxygen atoms in the surface structure, the highest oxidation state of the metallic species presents on the anode surface, or a combination of both factors is responsible for the absence of robust binding sites on metal oxides [67]. Additionally, compared to those corresponding to active electrodes, non-active anodes have higher oxygen evolution potential. Thus, for non-active electrodes, potential values vs. SHE in the range of 1.9–2.6 V are normal [64]. The boron-doped diamond (BDD) and titanium dioxide (TiO_2) electrodes are commonly used electrodes of this type, along with lead (iv) oxide (PbO_2), tin (iv) oxide (SnO_2), and titanium heptoxide (Ti_4O_7). The substrates require higher potential to overcome the activation energy required to generate molecular oxygen. This increases the rate of •OH radical production [45,68]. As the pathways for oxygen evolution and organic oxidation run concurrently, numerous anodes display a blended or mixed behavior [69].

2.2. Electro-Fenton Process

In the AO process, the anode material surface undergoes the oxidation of interfacial bulk solution, resulting in the production of •OH species. These radicals are highly reactive but have short half-life times, typically lasting around 10^{-9} s, which restricts their ability to oxidize substances to the immediate surroundings of the anode surface [38]. In contrast, Fenton mixtures promote reactions that produce •OH radicals throughout the entire volume of contaminated aqueous solutions, potentially making them more effective for treating wastewater. The Fenton reagent, composed of a combination of H_2O_2 and Fe^{2+} ions, triggers the generation of •OH radicals, as outlined in Equation (8).

$$Fe^{2+} + H_2O_2 \rightarrow Fe^{3+} + \cdot OH + OH^- \tag{8}$$

Despite the widespread use of Fenton processes to break down organic pollutants in water, several researchers [46,70] have emphasized three significant disadvantages. The first drawback pertains to the high cost associated with continuously adding H_2O_2 to the wastewater solution. The remaining two issues are associated with the costs incurred in neutralizing the treated effluent under acidic conditions (Equation (8)) and the management of separation and disposal of the sludge of ferric hydroxide generated in the neutralizing reaction phase [71,72].

To eliminate the necessity for the constant addition of H_2O_2 in wastewater solutions, one approach is to electrochemically produce the oxidant by utilizing the dissolved oxygen in the wastewater sample. The electrochemical-Fenton process, also known as electro-

Fenton, involves the reduction in dissolved O_2 in the presence of Fe^{2+} ions, as illustrated in Equation (9) [41].
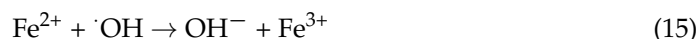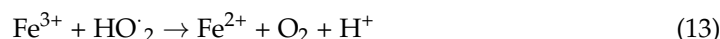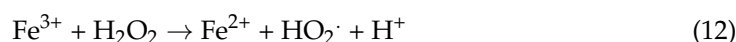
$$O_2 + 2H^+ + 2e^- \rightarrow H_2O_2 \tag{9}$$

The EF process requires an acidic environment to prevent precipitation, as indicated in Equation (8). Various research has mentioned that Fenton reaction occurred ideally at pH 3, leading to the prevalence of the $Fe(OH)^{2+}$ species as a primary source of Fe^{3+} compounds, as illustrated in Equations (10) and (11). The reduction in $Fe(OH)^{2+}$ at this pH results in the generation of Fe^{2+} [70,73].

$$Fe^{3+} + H_2O \rightarrow Fe(OH)^{2+} + H^+ \tag{10}$$

$$Fe(OH)^{2+} + e^- \rightarrow Fe^{2+} + OH^- \tag{11}$$
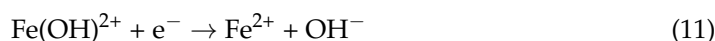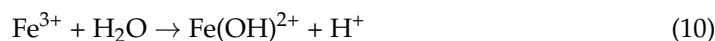
The EF method offers an additional notable advantage over the conventional Fenton approach, which lies in the significant presence of H_2O_2 at the boundary of the electrodes and wastewater sample. In this specific region, Fe^{3+} can be easily reduced to Fe^{2+} (Equation (12)), and a series of reactions (Equations (13)–(16)) generates different species with distinct oxidation potentials. Consequently, the continuous Fenton reagent production is facilitated and maintained through the cathodic regeneration of Fe^{2+} achieved by the electro-reduction in Fe^{3+} in the reactions [38,68,74].

$$Fe^{3+} + H_2O_2 \rightarrow Fe^{2+} + HO_2^{\cdot} + H^+ \tag{12}$$

$$Fe^{3+} + HO^{\cdot}_2 \rightarrow Fe^{2+} + O_2 + H^+ \tag{13}$$

$$H_2O_2 + {}^{\cdot}OH \rightarrow HO_2^{\cdot} + H_2O \tag{14}$$

$$Fe^{2+} + {}^{\cdot}OH \rightarrow OH^- + Fe^{3+} \tag{15}$$

$$Fe^{3+} + R^{\cdot} \rightarrow Fe^{2+} + R^+ \tag{16}$$

As demonstrated by Equations (14) and (15), both H_2O_2 and Fe^{2+} can serve as scavengers for •OH radical species. Consequently, it is essential to prevent an excess of the constituents of the Fenton reagent [41]. The outcomes are significantly influenced by the characteristics, makeup, and electrolytes present in the wastewater sample. The concentration of Fe^{2+} ions and electro-generated H_2O_2 from a saturated O_2 solution seem to establish a reasonable correlation. Notably, Brillas and his team have extensively studied the EF approach for the treatment of wastewater from the 1990s onward, affirming its effectiveness in degrading diverse pollutant types [44,74].
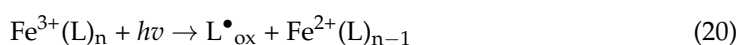
2.3. Photo Electro-Fenton Process

The photo electro-Fenton (PEF) technique involves illuminated systems where the electrochemical generation of H_2O_2 takes place in the existence of Fe^{2+} ions [75]. The simultaneous utilizing of electrical and radiation stimulation leads to the generation of a greater quantity of •OH compounds in comparison to conventional EF processes [76,77]. This enhanced generation of •OH radicals expedites the mineralization process of organic contaminants. For instance, in the case of organic pollutant mineralization, the PEF process achieved a total organic carbon (TOC) removal of over 90% within 180 min, while EF alone achieved 70% removal [75]. Pioneering research in this field was conducted by Brillas et al. [74], who significantly improved the degradation of aniline through EF treatment by illuminating the system with a UVA lamp (λ = 360 nm), resulting in an increase in TOC removal from 63% to 92%.

The positive impacts of UVA radiation can be attributed to two main factors. Firstly, UVA radiation facilitates the increased regeneration of Fe^{2+} ions from Fe^{3+} (Equation (12)). This regeneration process promotes the Fenton chemistry (Equation (8)), leading to the generation of a higher quantity of •OH radicals [41]. Secondly, UVA radiation facilitates the homogeneous generation of •OH radicals through the photochemical reduction in

ferric hydroxy complexes ($Fe(OH)^{2+}$) (Equation (17)) [47]. In addition, UVC radiation at a wavelength of 254 nm can also induce the photolysis of H_2O_2 compounds, leading to the generation of additional •OH species (Equation (18)) [75].

$$Fe(OH)^{2+} + hv \rightarrow Fe^{2+} + {}^{\bullet}OH \tag{17}$$

$$H_2O_2 + hv \rightarrow 2HO^{\cdot} \tag{18}$$

Moreover, the presence of electromagnetic radiation serves multiple purposes. It not only enhances the photo-generation of •OH agents but also triggers the photolysis of complexes involving carboxylic acids and Fe^{3+}. This photolysis process facilitates the regeneration of Fe^{2+} cations and promotes the occurrence of the photodecarboxylation reaction (Equation (19)) [75,78].

$$2Fe(C_2O_4)_n{}^{(3-2n)} + hv \rightarrow 2Fe^{2+} + 2CO_2 + (2n-1)C_2O_4{}^{2-} \tag{19}$$

$$Fe^{3+}(L)_n + hv \rightarrow L^{\bullet}_{ox} + Fe^{2+}(L)_{n-1} \tag{20}$$

As Brillas [79] explained, the irradiation of EF cells serves multiple beneficial purposes. Further to enhancing the photoreduction of ferric carboxylate complexes, resulting in an increased mineralization percentage, it also contributes to the improved generation of •OH radicals through the reproduction of ferrous ions and the photolysis of H_2O_2.

2.4. Solar Photo Electro-Fenton Process

UVA lamps have been extensively utilized among artificial lamps in the PEF system [44,78,80]. However, these lamps in the PEF technique often result in high electricity costs. To mitigate this, the solar photo electro-Fenton (SPEF) process offers a solution that takes advantage of a free source of ultraviolet radiation. The SPEF process always exhibits a higher rate of mineralization of organic pollutants compared to the PEF approach [75]. This is primarily attributed to the higher UV intensity of sunlight within the visible region ($\lambda > 400$ nm) [38,75]. Consequently, this combination facilitates the direct ferric carboxylate complexes photolysis, as described in Equation (20).

SPEF demonstrated remarkable efficacy in achieving high degradation percentages of organic contaminants, reaching up to 100% within shorter timeframes in comparison to PEF [81]. Additionally, it exhibited high rates of mineralization, with TOC elimination ranging between 70 and 99% [38]. An important advantage of SPEF is its ability to significantly reduce energy consumption without compromising degradation efficiency. Some researchers reported a substantial decrease in energy requirements of up to 85%, making the utilization of sunlight in these technologies a promising approach for organic contaminant elimination from waste streams [82,83].

3. Reactors Used for EAOPs

The ability of EAOPs to undergo oxidation is influenced by the reactor design, the electrodes used, the applied current density, the UV light source, etc. The procedures outlined in this analysis were carried out using compact laboratory-scale arrangements. Consequently, additional in-depth research is required for upscaling these processes to an industrial magnitude. This upscaling is crucial for addressing overarching concerns, including the assessment of costs and the optimization of operational parameters.

3.1. Reactors Used for AO Process

To create an effective electrochemical reactor, some strategies must be taken into account. Initially, the design of reactors should adhere to the electrocatalysis requirements. Secondly, the assembly process should be highly feasible, meaning that the configuration, operation, and maintenance of the reactor need to be kept as simple as possible [84]. Additionally, the materials used for the electrodes should be easily accessible and cost-effective. Lastly, the reactor itself should possess good versatility and prioritize environmental friend-

liness [85]. The classification of electrochemical reactors will be based on factors such as the design of the reactor, mode of operation, flow mode, and arrangement of electrodes.

Most of these systems comprise cylinder-shaped tank reactors and reaction chambers equipped with working and reference electrodes, functioning as undivided configurations. Undivided reactors circumvent the possible repercussions of the membrane and decrease in the electrical expenses in comparison with divided reactors [66]. However, in divided reactors, the membrane separator can control the movement of ions throughout the anolyte and catholyte chambers. Lee et al. [86] constructed a double chamber reactor for electro-stripping ammonia recovery from DW (Figure 2). They used Nafion-117 as a cation exchange membrane (CEM) to divide the anode and cathode chamber, helping to obtain charge neutrality and capture ammonia gas in sulfuric acid solution as ammonium sulfate fertilizer. However, membrane-based reactors faced some problems during treatment operation. The major drawback was the fouling of membrane pores with suspended particles in the DW, which can decrease membrane permeability. The replacement of the membrane can increase overall treatment costs. There is a scope of further research to remediate fouling problems during treatment time.
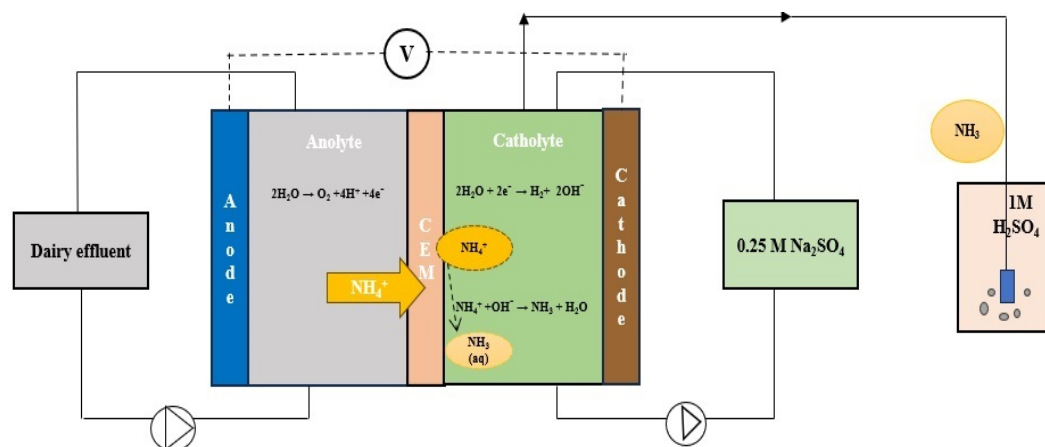

Figure 2. Dual chambered electrochemical ammonia stripping process employing a cation exchange membrane (CEM) to separate anolyte and catholyte chambers from dairy wastewater treatment (Adapted with permission from Ref. [86]. 2021, Lee et al.).

Most researchers have limited the capacity of their EAOPs reactors to within 1 L (Tables 1 and 2). Li et al. [87] utilized a novel approach in regard to the one liter capacity, incorporating ultrasound assisted electro-oxidation to recover heavy metals from DW (Figure 3). They used a salt bridge to connect two cuvettes containing electrodes. The ultrasonic generator stimulated the oxidation process by generating hydroxyl compounds. An Ag/AgCl electrode is incorporated as a reference electrode to maintain a constant anodic potential through the potentiostatic operation. However, undivided reactors are preferred as they eliminate the potential drawback associated with the membrane or separator, consequently reducing the cost of energy of the reactor [47]. As an advanced treatment approach, pre-ozonation exhibits good removal performance when it is integrated with the AO process. Alfonso-Muniozguren et al. [88] designed a pre-ozonation-based photoreactor which connected with an electrochemical cell consisting of Ni/BDD anodes and platinum cathodes (Figure 4). The AO performance was increased by adding H_2O_2 and UVC light. This combined system achieved good degradation efficiency of slaughterhouse wastewater treatment [88]. AO integrated biological approaches occasionally perform well in regard to nutrient removal and recovery from DW. Ding et al. [89] designed an electrochemical reactor coupled with an up-flow anaerobic sludge blanket (UASB) unit to recover phosphorous from DW (Figure 5). They also found this technology to be efficient for biogas production as an alternative energy source.

Table 1. Dairy wastewater treatment studies based on anodic oxidation (AO) mechanism.

Process	System Configuration	Electrode Used (Anode-Cathode)	Optimal Experimental Conditions	Removal Efficiency	Highlights of the Research	References
Electrochemical Stripping	Dual chamber reactor, Volume: 150 mL, 0.25 M Na_2SO_4, CEM: Nafion-117	Pt-Pt	Current density: 93.8 mA/cm^2, Treatment time: 400 min	TAN (real WW): 17,704 mg-N/L; and TAN (synthetic WW): 10,158 mg-N/L	The swift buildup of NH_3 provided feasibility for its ongoing operation.	[86]
Ultrasound assisted EO	Volume: 120 mL, Electrolyte: NaCl	Ru–Ir/Ti, Ag–AgCl	Treatment time: 45 min; Power of ultrasonic: 400 W; NaCl: 10 g/L.	Cu: 96.8%, Zn: 98.5%	The findings found this approach is a novel and effective technique. It offers speed and convenience while ensuring efficient digestion, making it highly promising for various applications.	[87]
EO/UVC/H_2O_2	Volume:1.4 L, UVC lamp power: 11W, Effective area of electrodes: 10 cm^2, Interelectrode gap: 3.7 mm	BDD-Pt	H_2O_2: 850 mg/L, Current density: 100 mA/cm^2, O_3:100 mg/L, Flow rate of gas: 0.3 L/min, Treatment time: 120 min	Color: 100%, TOC: 100%	By transforming the original organic molecules into quickly oxidizable chemicals, the pre-ozonation phase enhanced the removal of organics by EO and other associated processes.	[88]
EO-UASB	Volume: 150 mL, Effective area of electrodes 26.2 and 52.5 cm^2	SS-SS	Treatment time: 36 days, applied voltage: 1 V	TP: 65.1% CH_4: 10.9%	The electrochemically enhanced UASB approach has the capability to generate increased biogas while minimizing H_2S content and retrieving phosphorus-enriched sludge.	[89]

Table 1. *Cont.*

Process	System Configuration	Electrode Used (Anode-Cathode)	Optimal Experimental Conditions	Removal Efficiency	Highlights of the Research	References
EO	Volume: 150 mL, Interelectrode gap: 1.5 cm, Effective area of electrodes: 12.5 cm^2	Pt/Ti or IrO$_2$/Ti or IrO$_2$-Pt/Ti-Zirconium bar	Current density: 100 mA/cm^2, Treatment time: 360 min, NaCl: 0.2 M, Temperature: <40 °C	COD: 100%, Color: 100%	The IrO$_2$/Ti anode excels over Pt/Ti or IrO$_2$-Pt/Ti anodes at reduced applied current, whereas Pt/Ti anode demonstrates superior COD removal at elevated current density.	[90]
EO	Volume: 500 mL, Interelectrode gap: 1.0 cm, Effective area of electrodes: 33 cm^2	Ti/Pt-IrO$_2$-SS	Treatment time: 300 min, Current: 1A, NaCl: 1%	TOC: 51.4%, NH$_3$-N: 100%	Ti/Pt-IrO$_2$-SS exhibited feasibility without pretreatment of the effluents.	[91]
EO	Volume: 1L, Recirculation Flow Rate: 194.4 L h^{-1}, COD$_o$ = 3350 mg/L	BDD-BDD	Current density: 357 A/m^2, Treatment time: 360 min	COD: 88%	Specific energy consumption: 137 Wh gCOD^{-1}	[92]
EO	Volume: 5 L; Electrolyte: Na$_2$SO$_4$ and FeCl$_3$, COD$_o$ = 4950 mg/L	BDD-BDD	Current density: 7.7 mA/cm^2, Treatment time: 300 min, pH: 6.6	COD 82.5%, turbidity 76%, and color 83%	The inclusion of identical supporting electrolytes has resulted in improved removal of turbidity and color.	[93]
EO	Volume: 1L, Recirculation Flow Rate: 194.4 L h^{-1}, COD$_o$ = 2280 mg/L	BDD-BDD	Current density: 357 A/m^2, Treatment time: 180 min, pH: 6.6	COD: 85%	Specific energy consumption: 100 Wh gCOD^{-1}	[94]
EO	Volume: 2L; Interelectrode gap: 8 cm; Electrolyte: NaCl;	Carbon-Fe/SS	Applied voltage: 11.29 V; Electrolysis time: 8h.	COD: 53.33%	The findings of this study demonstrate the viability of utilizing electrochemical treatment for whey wastewater as a viable alternative to traditional conventional methods.	[95]

Process	System Configuration	Electrode Used (Anode-Cathode)	Optimal Experimental Conditions	Removal Efficiency	Highlights of the Research	References
EC + EO	For EC: Volume: 1 L; Interelectrode gap: 5 cm. For EO: Volume: 0.5 L; Interelectrode gap: 0.5 cm; COD_o = 3850 ppm	EC: Al-Al, EO: Ti/Pt-Ti/Pt	For EC: Current density: 0.6 A/dm^2 and Electrolysis time: 6 min For EO: Current density:1.4 A/dm^2 and Electrolysis time: 15 min	COD: 66.4%, Color: 90.4%, Turbidity: 100%	The utilization of the seed toxicity test enables the assessment of the efficiency and quality of the investigated effluent treatment system. Results indicated that seeds irrigated with either untreated waste or treated dairy effluent do not exhibit any phytotoxic effects.	[96]
Hybrid EC-EO system	Volume: 500 mL; Interelectrode gap: 7.5 cm; Electrolyte: NaCl;	EC: Al-Fe; EO: TiO_2-Al/Fe	Bipolar connection: Electrodes: TiO_2-Al, Current applied: 3 A, Treatment time: 100 min, Monopolar connection: Electrodes: TiO_2-Fe, Current applied: 3.0 A, Treatment time: 60 min	COD: 78.21%, and Turbidity: 94.52%, COD: 50.19%, and Turbidity: 90.22%	The monopolar connection mode resulted in minimal metal dissolution levels, while the bipolar connection mode was determined to be more expensive compared to the monopolar mode.	[97]
UV assisted EO	Volume: 250 cm^3, Interelectrode gap: 1 cm	$Ti/Ru_{0.3}Ti_{0.7}O_2$ mesh-Ti plates	Current: 533.42 mA, λ_{max}: 254 nm, Treatment time:120 min	COD:97.80%, TOC: 94.62%	The effectiveness of the $EC/UV/Cl_2$ technique can be ascribed for photolysis of active chlorine compound, resulting in the generation of extremely reactive radicals.	[98]
EO	Volume: 700 mL; Interelectrode gap: 3 mm	Ti/Pt mesh-Ti mesh	current density: 4.73 mA/cm^2, NaCl: 0.025 M, pH:7.03, Reaction time: 4 h	COD:93.1%, TOC:89.0%, TSS: 99.5%, TN:93.6%, color: 100%. And Energy consumption: 154.0 kWh/m^3 and 15 kWh/kg COD	Further advanced treatment process was suggested to reduce the treatment time.	[99]

Process	System Configuration	Electrode Used (Anode-Cathode)	Optimal Experimental Conditions	Removal Efficiency	Highlights of the Research	References
EC + EO	Volume: 800 mL (EC), 150 mL (EO); Electrolyte: NaCl and Na_2SO_4; Interelectrode gap: 1 cm	EC: Al-Fe (mesh) EO: Ti/IrO_2–Ta_2O_5–Pt wire	For EC: Current density: 9.09 mA/cm^2; Electrolysis time: 120 min; For EO: Mixing speed: 800 rpm;	For EC: Turbidity: 90%, COD: 81%; Combined EC + EO: TOC: 98%	Chlorinated species showed better mineralization of pollutants than Na_2SO_4	[100]
EC + EO	Volume: 500 mL; Interelectrode gap: 1 mm	EC: Al/Fe-Al/Fe, EO: Ti/RuO_2-TiO_2-SS, Ti/IrO_2-Ta_2O_5-SS	Current density: 20 mA/cm^2; Electrolysis time: 5 h;	TN:91%, COD: 85%, TOC: 93%, and TP: 76%	Significant removal of pollutants was successfully accomplished through the implementation of these integrated processes.	[101]
Electrochemical Stripping	Volume: 35 mL Electrode area: 25 cm^2, Membrane surface area: 71.4 m^2/m^3, AEM: FAA-3-PK, CEM: Nafion-115	Carbon cloth-SS	Current density: 30 A/m^2, Treatment time: 4 h.	NH_4^+: 83.5–99.6%	The application of cathode-fed reactor with a chlorine trap to treat dairy effluents offers various merits and creates the potential for scaling up the entire system.	[102]
EC + PEF + EO	Volume: 100 mL Interelectrode gap: 1.0 cm	EC: Fe-Al, PEF: Pt-SS, EO: DSA-BDD	For EC: Current density: 30 mA/cm^2, Treatment time: 60 min; pH: 3.0, For EO + PEF: Current density: 50 mA/cm^2, Treatment time: 480 min	TOC: 22–27% (EC); 49.1% (EO + PEF)	This research suggested that solar assisted PEF is a cost-effective approach in terms of energy consumption in comparison to UVA lamp assisted PEF.	[103]
EC + EO	Volume: 500 mL; Dimension of electrode: 10 cm × 5 cm × 0.3 cm; Effective area of electrode: 20 cm^2; Interelectrode gap: 0.5 cm;	EC: Al-Al, EO: BDD-Graphite	Agitation speed: 300 rpm; Current density: 200 A/m^2, Treatment time: 2 h, Dilution ratio: 1:5.	P-PO_4: 100%, COD: 70%, N-NO_3: 80%, and TN: 20%.	Combined process increased pollutant removal compared to a single EC process.	[104]

Table 1. *Cont*.

Process	System Configuration	Electrode Used (Anode-Cathode)	Optimal Experimental Conditions	Removal Efficiency	Highlights of the Research	References
EO	Interelectrode gap: 1 cm Electrode dimension: 100×50 mm	DSA ($RuO_2 + IrO_2$)–SS Ti/PbO_2–SS	Treatment time: 540 min, Applied current: 1.5 A, and NaCl: 0.5 g,	COD: 32% NH_4-N: $\approx$100% COD: $\approx$60% NH_4-N: $\approx$90%	The findings demonstrated that the addition of NaCl and suspended particles filtering as a pretreatment might enhance the overall efficiency of NH_4-N removal from the digested effluent during electrochemical oxidation.	[105]
EO	Volume: 1000 mL, Interelectrode gap: 1 cm, Dimension of electrodes: 15 cm $\times$ 4 cm$\times$ 0.3 cm, Effective area of electrodes: 20 cm^2	Ti/IrO_2–SS	Current density: 0.044 A/cm^2, Treatment time: 240 min, NaCl dose: 3.87 g/L	TN: 100%, Color: 100%	Future study may be needed to investigate cathodic reduction in NOx-N with regard to nitrite and nitrate individually.	[106]

Table 2. Electro-Fenton (EF), photo electro-Fenton (PEF), and solar photo electro-Fenton (SPEF) approaches for dairy wastewater treatment.

Process	System Configuration	Electrode Used (Anode-Cathode)	Optimal Experimental Conditions	Removal Efficiency	Highlights of the Research	References
EF	Volume: 1 L, Dimension of the electrodes: 15 cm $\times$ 5 cm $\times$ 1 mm, Effective area of electrodes: 60 cm^2	Ti-RuO_2-Carbon Felt, Ti-P_dPtOx-Carbon Felt, BDD-Carbon Felt	Treatment time: 60 min, Current density: 2.5 mA/cm^2, Fe^{2+}: 41.20 mg/L, Mixing speed: 350 rpm, pH: 3.5, and Temperature: 23 °C	COD: 83.5% (Ti-RuO_2-Carbon Felt); 77.9% (Ti-P_dPtOx-Carbon Felt); and 74.3% (BDD-Carbon Felt)	This study confirms that the degradation trends are influenced by the generation of $\bullet$OH which varies across different types of anodes.	[107]
EF + AO	Volume: 2 L, Electrode dimension: 10 cm $\times$ 10 cm, Na_2SO_4: 0.1 M, and Initial pH: 3	PbO_2-modified graphite	Electrolysis time: 80 min, Fe^{2+}: 0.3 mM	COD$_{Cr}$: 71.5%	The electron paramagnetic resonance (EPR) technique effectively captured the generated hydroxyl radicals. The innovative electrolysis system enhances the wastewater's biodegradability by 400%.	[108]

Table 2. *Cont.*

Process	System Configuration	Electrode Used (Anode-Cathode)	Optimal Experimental Conditions	Removal Efficiency	Highlights of the Research	References
EF + SBR	Volume: 10 L, Dimensions of the electrodes: 5 cm $\times$ 5 cm $\times$ 0.5 cm, Interelectrode gap: 5 cm, Flow rate of O_2: 2 mg/L	Fe-Fe	EF treatment time: 120 min, Current density: 2.0 mA/cm^2, H_2O_2: 1 mM, and pH: 5	COD: 99%, TN: 97%, and TP: 95%	This newly developed system demonstrates economic viability and outperforms conventional biological treatment systems.	[109]
SPEF	Volume: 2.5 L, HRT: 24 h, OLR: 3.94 and COD: 8.15 g L^{-1} d^{-1}	Ti/Ru$_{0.3}$Ti$_{0.7}$O$_2$-GDE	Treatment time: 300 min, Fe^{2+}: 1 mM pH: 3; Current density: 10 mA/cm^2, Temperature: 31 °C, UVA radiation: 37 W/m^2	COD: 88%, and Turbidity: 80%	SPEF exhibited complete contaminants mineralization and very cost-effective approach as they used sunlight for photo chemical reduction.	[110]
EF	Volume: 250 mL, Interelectrode gap: 3 cm, Dimension of the electrodes: 2.0 cm $\times$ 0.5 cm, and Effective area of electrodes: 1.0 cm^2	Fe-Fe	Current density: 56 mA/cm^2, Treatment time: 90 min, H_2O_2/Fe^{2+} molar ratio: 3.965, H_2O_2: 0.898 mL/L, pH: 7.52	COD: 93.93%, Color: 97.32%	The findings found efficient treatment approach for pollutant removal from dairy waste stream.	[111]
EF	Volume: 400 mL, Dimension of the electrodes: 2.0 cm $\times$ 0.5 cm, Interelectrode gap: 3.0 cm, Effective area of electrodes: 1.0 cm^2	Fe-Fe	pH: 7.58, Treatment time: 87.13, Current density: 58.5 mA/cm^2, H_2O_2/Fe^{2+} molar ratio: 3.62, H_2O_2/DW: 1.39 mL/L	COD: 93.24%	This study suggested graphite electrodes covered with different oxidant nanoparticles could be employed to enhance the generation of hydroxyl radicals, playing a crucial role in this procedure. Additionally, alternative energy sources like sunlight can potentially decrease energy cost.	[112]
EF	Volume: 2 L, Dimension of the electrodes: 7 cm $\times$ 10 cm $\times$ 0.3 cm,	Graphite-Graphite	Fe^{2+}: 0.0625 mol, H_2O_2/Fe^{2+} molar ratio: 14.48, Current density: 9.68 mA/cm^2	COD: 86.75%, EC: 0.36 kWh/kg COD, CE: 47.11%	The findings indicated the current treatment, utilizing affordable graphite electrodes, produced highly competitive and encouraging outcomes, particularly in conditions of low current density.	[113]

Process	System Configuration	Electrode Used (Anode-Cathode)	Optimal Experimental Conditions	Removal Efficiency	Highlights of the Research	References
EF	Volume: 500 mL, Dimension of the electrodes: 6 cm × 11.5 cm× 0.1 cm, Interelectrode gap: 2 cm, Effective area of electrodes: 46.2 cm^2	Fe-Fe	Current density: 32 mA/cm^2, H_2O_2/COD:2, Treatment time: 45 min, and pH: 2.4	COD: 72%, orthophosphate: 88%, SS: 88%, Color: 88%	The removal of COD rose with higher H_2O_2/Fe^{2+} ratios and prolonged treatment times, while it decreased with elevated H_2O_2/COD ratios and pH.	[114]
EF + AD	Volume: 5000 mL, Electrode area: 28 cm^2, Mixing speed: 150 rpm	Fe-Fe	Treatment time: 50 min, Current density: 9 mA/cm^2, Flow rate: 40 mL/min, Temperature: 50 °C, pH: 6, H_2O_2/Fe^{2+} molar ratio: 0.8	Turbidity: 93%, COD: 97%	Combined methods showed better removal performance than any single method	[115]
AD + SPEF	Volume: 100 mL, Na_2SO_4: 0.05 M, $FeSO_4$ $7H_2O$: 1.0 mM, Effective area of electrodes: 2.5 cm^2, Interelectrode gap: 0.5 cm, Air flow rate: 1.0 L/min	Si/BDD-carbon-PTFE-GDE,	Current density: 50 mA /cm^2, Treatment time: 180 min, pH: 3, Temperature: 35 °C, Na_2SO_4: 0.05 M, H_2O_2: 11.62 mM, UV radiation: 19 W/m^2	COD: 99.3%, TOC: 99.2%, TSS: 100%, color: 100%, BOD_5: 99.1%, and Turbidity: 99.6%.	After a span of 30 days, there was a generation of 90 mL of methane.	[116]
EF + AD	Volume: 340 mL Electrode area: 2.5 cm^2, active area of 60 cm^2,	Si/BDD-GDE	Treatment time: 180 min, pH:3.0	COD: 97%, CH_4: 90 mL, Current densities: 30–50 mA/cm^2	The integrated approaches resulted in a complete degradation of organic pollutants from dairy waste stream.	[117]
EC + EF/PEF	EC reactor: 175 mL, EF/PEF: 150 mL Interelectrode gap: 1 cm, electrode area: 3 cm^2,	EC: Fe-Fe, EF/PEF: Si/BDD-GDE, or RuO_2-GDE	Agitation speed: 800 rpm, pH: 3.0, UVA irradiation: 5 W/m^2, Air flow rate: 1 L/min,	Lactic acid bacteria: 100%, *E. coli*: 100%, and Enterococci bacteria: 100%	PEF process showed better performance than EF approach	[118]

Table 2. *Cont.*

Process	System Configuration	Electrode Used (Anode-Cathode)	Optimal Experimental Conditions	Removal Efficiency	Highlights of the Research	References
PEF, SPF, and FSPF	Volume: 1 L, UV lamp: 20 W, Electrode dimension: 15 cm $\times$ 5 cm $\times$ 1 mm	Ti-RuO$_2$-Carbon felt	Treatment time: 60 min, Current density: 2.5 mA/cm^2, Fe^{2+}: 28.0 mg/L, UV applied: 950 W/m^2, and Initial pH: 3	COD: 92–95%	The applicability of the three processes is feasible, and when making a decision, additional factors such as water usage, treatment duration, infrastructure expenses, operational expenses, and remaining iron concentrations in the solution should be taken into account.	[119]
EC+ PF	Volume: 200 mL, Fe^{2+}: 198 mg/L, and H$_2$O$_2$: 14,000 mg/L, NaCl: 0.5 g	Al-Fe	Current density: 85.71 A/m^2, Treatment time: 35 min, pH: 2.95	COD: 92.2%, TOC: 89.9%	The overall operational expense for the treatment amounted to $48.05 per kg of COD removal. Specifically, the UV/Fe^{2+}/H$_2$O$_2$ pretreatment incurred $39.36 per kg of COD removal, while the EC post-treatment cost was $8.69 per kg of COD removal.	[120]
EF	Volume: 1.5 L Dimensions of the electrodes: 10 cm $\times$ 8.5 cm, Interelectrode gap: 1.0 cm, and Effective area of the electrodes: 161.5 cm^2	Fe-Fe	Treatment time: 50 min, Current density: 27 mA/cm^2, pH: 7	COD: 70%	To comprehend the electrochemical mechanism and investigate the disposal of generated residues, a physico-chemical examination of iron electrodes and the resulting scum and sludge was conducted.	[121]
CC-EF	Volume: 1 L, Dimensions of the electrodes: 10 cm $\times$ 8.5 cm,	Fe-Fe	PAC: 100 mg/L, Voltage: 20 V, H$_2$O$_2$: 1.5 g/L, Treatment time: 60 min, pH: 3, and Interelectrode gap: 2 cm	COD: 90.3%, BOD$_5$: 87.25%, and TSS: 87%	This integrated process presents an intriguing approach for the treatment of dairy effluents, with the Feed forward Artificial Neural Network model proving to be a more effective tool compared to the Partial Least Squares model.	[122]

Table 2. *Cont*.

| Process	System Configuration	Electrode Used (Anode-Cathode)	Optimal Experimental Conditions	Removal Efficiency	Highlights of the Research	References
EF	Volume: 3 L, Effective electrode: 1.5 cm	Fe-Al	pH: 5.95, Treatment time: 60 min, H_2O_2 = 1.5 mL, H_2O_2/Fe^{2+}: 1.8	COD: 95.8%, Turbidity: 97.2%	More effective materials such as metal-organic frameworks were suggested for further study.	[123]
EC+EF	Volume: 350 mL, Effective area of the electrodes: 100 cm^2	Al-Fe	Current density: 15 mA/cm^2; H_2O_2: 3000 mg/L;	COD: 79.2%	Only 20 min treatment times exhibited good COD removal efficiency.	[124]
CC-EF	Volume: 500 mL Interelectrode gap: 1 cm	Fe-Fe	PAC: 75 mg/L, Voltage: 20 V Treatment time: 75 min, H_2O_2: 2500 mg/L, pH: 3	COD: 89.55%, BOD: 88.88%, TSS: 91.27%, TKN: 69.23%, and FC: 100%	Integrated chemical coagulation and electro-Fenton process found good pollutant removal efficiency in comparison to any single process	[125]
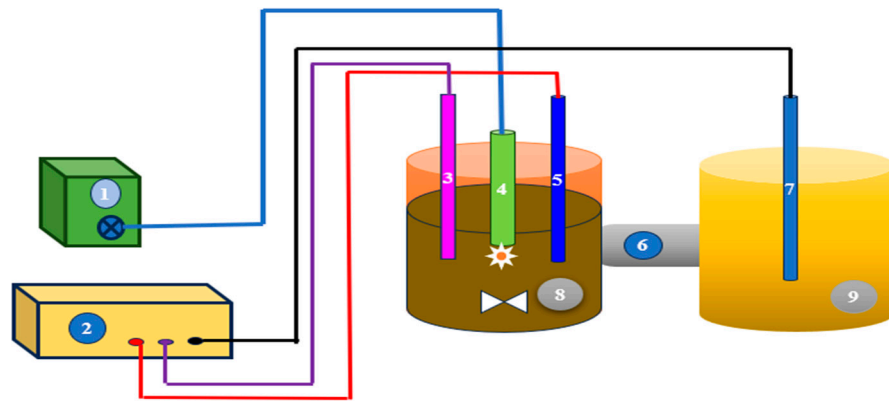
Figure 3. Ultrasound-assisted EO reactor for dairy wastewater treatment. 1. Ultrasonic. generator, 2. D.C. power supply, 3. Reference electrode, 4. Ultrasonic sensor, 5. Working electrode, 6. NaCl salt bridge, 7. Auxiliary electrode, 8. Digestion cuvette, and 9. Auxiliary cuvette (Adapted from Ref. [87]. 2021, Li et al.).
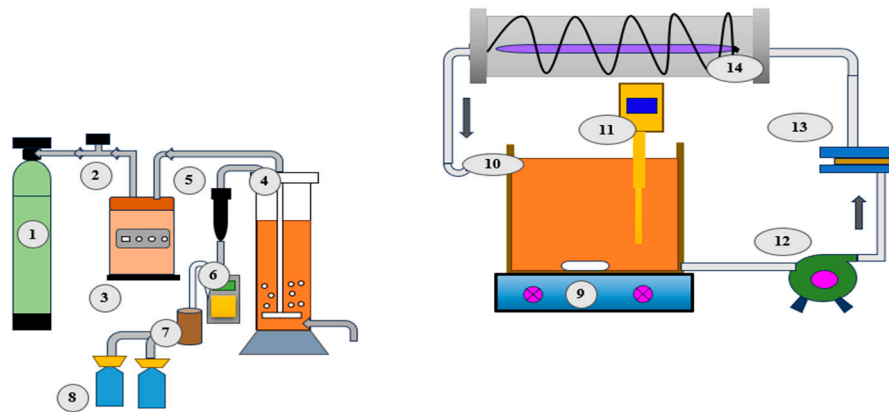

Figure 4. Combined pre-ozonization–electro-oxidation reactor for slaughterhouse wastewater treatment. 1. Oxygen bottle, 2. mass flow controller, 3. ozone generator, 4. ozonation column, 5. dehumidifier, 6. ozone analyzer, 7. heated catalyst, 8. KI 2% bottle, 9. magnetic stirrer, 10. recirculation vessel, 11. pH/temperature meter, 12. gear pump, 13. electrochemical cell, and 14. FluHelik reactor (Adapted with permission from Ref. [88]. 2020, Alfonso-Muniozguren et al.).
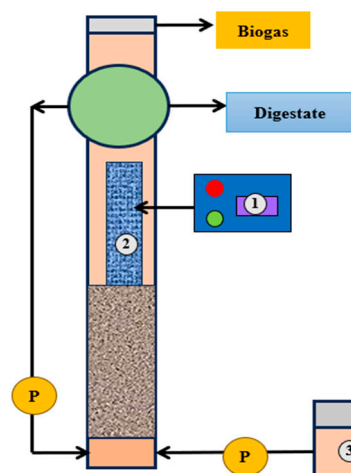

Figure 5. A unit of electrochemical coupled up-flow anaerobic sludge blanket reactor for phosphorous recovery from dairy wastewater. 1. DC power supply, 2. Stainless steel mesh electrodes, and 3. Liquid dairy manure (adapted with permission from Ref. [89]. 2021, Ding et al.).

Tank-type reactors are commonly utilized in EAOPs due to their versatility in adapting to various operating conditions. These reactors are typically small and cylindrical in shape, featuring a batch mode with magnetic stirring operating systems. Magnetic stirring serves multiple purposes, including the homogenization of the wastewater samples and increasing the diffusion–convection reagent mass transportation between the anodes and cathodes, as well as the removal of by-products from the system. Conversely, a distinctive three-electrode tank reactor designed for AO incorporates an internal rotary mixer for stirring, although its utilization in the literature is limited. Numerous tank reactors are equipped with jackets to uphold a consistent solution temperature, being managed through an external thermostatic water circuit. Maintaining control over temperature and adjusting pH are crucial prerequisites for precise kinetic analysis of pollutant degradation. For maintaining reaction temperature, a water-cooling jacket is encased around the reactor, as depicted in Figure 6 [126].
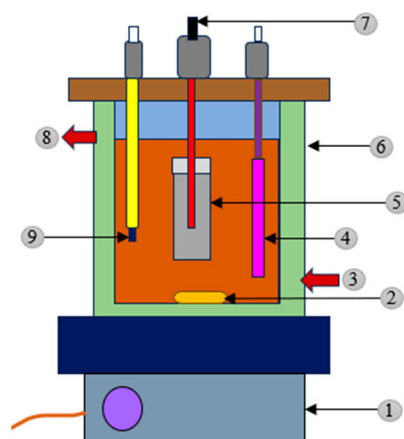

Figure 6. A BDD anode and graphite cathode contain water jacket surrounded AO reactor. 1. Magnetic stirrer, 2. magnetic bar, 3. water input, 4. BDD anode, 5. porous ceramic cylinder, 6. thermostatic cell, 7. graphite carbon bar cathode, 8. water output, and 9. pH meter (Adapted with permission from Ref. [126]. 2010, Samet et al.).

By comprehending the utilization of either divided or undivided reactors, depending on the suitability chosen (i.e., considering the significance of both cathodic and anodic reactions), it becomes feasible to regulate the reactor potential by incorporating or omitting a membrane or separator, thereby adjusting the generation of oxidants, electrical demands, and associated expenses accordingly. It is advised to carefully choose electrodes, particularly encouraging the exploration and experimentation with efficient materials on a large scale. When employing divided reactors, it is crucial to extensively research critical operational parameters, such as the materials employed for the cation exchange membrane, as well as the composition of water matrices. This thorough examination aims to gain a deeper understanding of the impact of side reactions, synergistic or antagonistic effects, and the generation of oxidative compounds in the AO process.

3.2. Reactors Used for EF, PEF, SFEF Processes

The design of EF reactors are similar to AO reactors; however, in photo-assisted reactor designs, there should be a natural or artificial UV light source. In Figure 7, an integral EF reactor was designed for removing pollutants from DW. In this reactor, Ti-PdPtOx and BDD electrodes were used as the anodes and carbon felt was used for the cathodes [107]. To maintain continuous electro-generation of H_2O_2 for Fenton reaction, air flow was ensured perpetually (Figure 7). A pH sensor was used to maintain the pH of the solution. Sometimes, the EF approach was coupled with other treatment approaches to increase the efficiency of the reactor. For example, Kuang et al. [108] integrated the EF process with the AO technique to improve the organic-pollutant removal efficiency from DW (Figure 8). In both approaches, they used PbO_2 as the anodes and modified graphite

felt for the cathodes. Heidari et al. [109] applied EF as a first step and a sequencing batch reactor (SBR) as a polishing step to increase the biodegradability of DW (Figure 9). They found this coupled system to be very efficient and economically feasible in comparison to other conventional biological treatment processes [109].
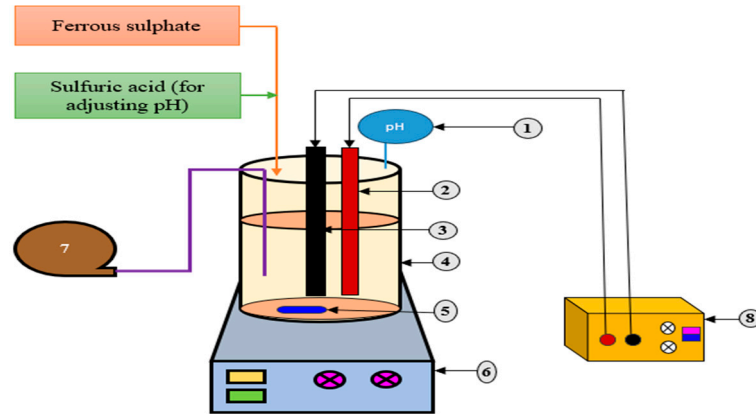

Figure 7. EF reactor using DSA/BDD anodes and carbon felt cathodes for treating DW. 1. pH sensor, 2. DSA/BDD anode, 3. carbon felt cathode, 4. reactor, 5. magnetic bar, 6. magnetic stirrer, 7. air pump, 8. DC power supply. (Adapted with permission from Ref. [107]. 2015, Paramo-Vargas et al.).
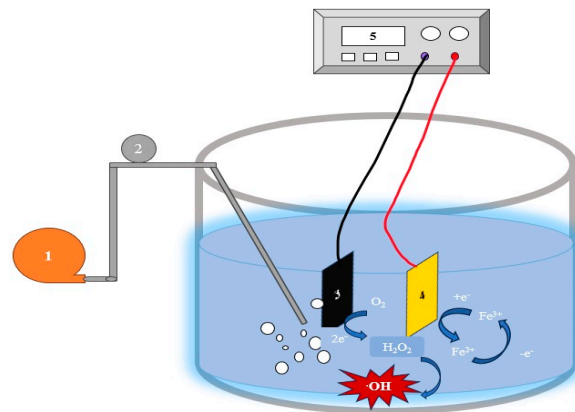

Figure 8. Integrated EF-AO for livestock wastewater treatment. 1. Air pump, 2. Air flow line, 3. Graphite felt cathode, 4. Modified PbO_2 anode, and 5. DC power supply (adapted with permission from Ref. [108]. 2019, Kuang et al.).
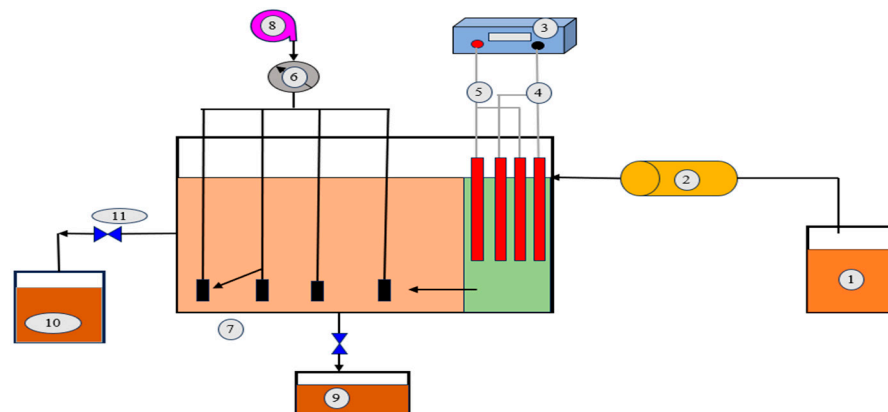

Figure 9. EF coupled with SBR for DW treatment. 1. Dairy wastewater, 2. peristaltic pump, 3. DC power supply, 4. anodes, 5. cathodes, 6. programmable timer, 7. air stones, 8. air pump, 9. waste sludge, 10. treated effluent, and 11. gate valves (Adapted from Ref. [109]. 2021, Heidari et al.).

The SPEF system has several advantages in comparison to the PEF system. One of the major benefits is utilizing solar energy, which reduces the cost of energy consumption of the system. Vidal et al. [110] integrated the SPEF system with a UASB biological approach to increase the degradation performance of the reactor to treat livestock waste streams (Figure 10). They achieved five times less operating expense for using sunlight for photochemical reduction in the pollutants [110].
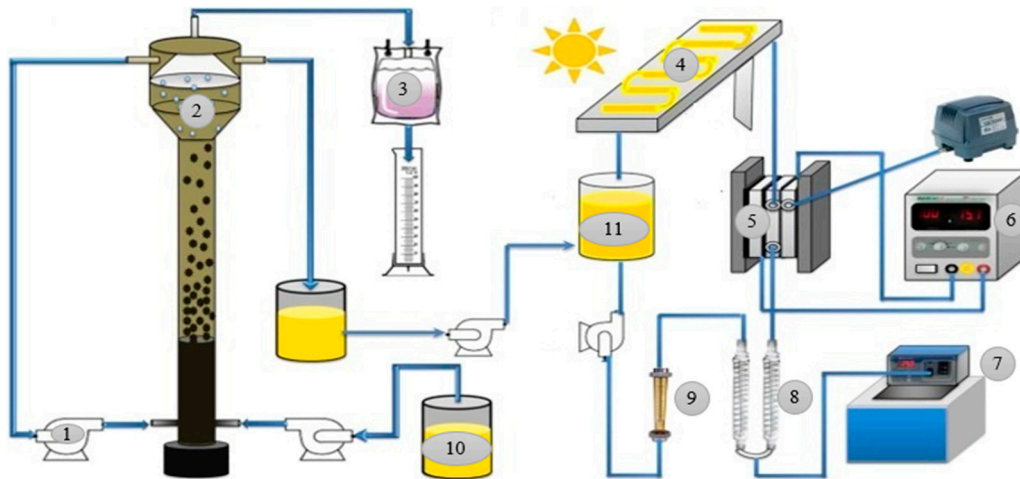

Figure 10. In integrated SPEF-UASB reactor employing solar energy for photo degradation of organic pollutants in wastewater. 1. Water pump, 2. USAB reactor, 3. Gas capture system, 4. Photovoltaic collector, 5. Electrochemical cell, 6. Power supply, 7. Thermoregulated bath, 8. Heat exchanger, 9. Rotameter, 10. Influent tank, and 11. Effluent tank (Adapted with permission from Ref. [110]. 2019, Vidal et al.).

The adaptability of PEF reactors contain UV lamps to stimulate ●OH radical generation for increasing pollutant removal efficiency. For such instances, Figure 11 illustrates the submersion of UVC light into the solution for photo-electrolysis with H_2O_2 electro generation [127]. Additionally, these reactors can be applied in hybrid processes. In two-electrode reactors, the operation revolves around supplying a consistent current through a power source. This establishes the voltage difference across the electrodes, which is crucial for calculating the energy consumption of the process [66].
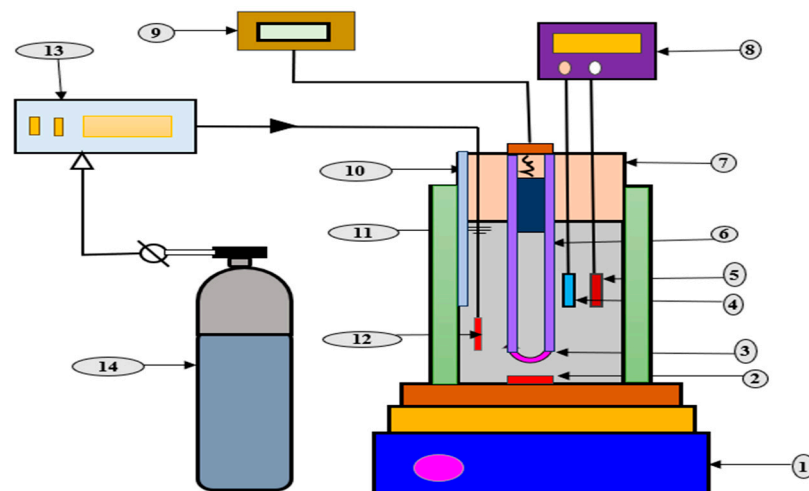

Figure 11. Photoreactor contains UV-C lamp and H_2O_2 generation set-up. 1. Magnetic stirrer, 2. stirring bar, 3. UV lamp, 4. anode, 5. cathode, 6. quartz jacket, 7. reactor, 8. DC power supply, 9. UV-power supply, 10. sampling port, 11. water bath, 12. bubble diffuser, 13. gas flowmeter, and 14. oxygen/air tank (adapted with permission from Ref. [127]. 2016, Frangos et al.).

When examining compact tank reactors, the primary emphasis should be on comprehending the efficacy of the treatment. This involves assessing its relative oxidation capability, exploring the kinetics of pollutant breakdown, evaluating the influence of operational parameters on degradation and mineralization processes, and identifying any resultant by-products [128–130]. However, it should be noted that determining treatment efficiency and energy consumption based on these data is not practical for industrial-scale applications due to the limited working volume. A more suitable approach for full-scale implementation is to consider flow systems, which allow for the treatment of larger solution volumes in batch mode [66].

This section highlights the various configurations explored for EF, PEF, and SPEF reactors, predominantly on a laboratory scale. It underscores the need for extensive research to comprehensively grasp the impact of numerous experimental variables on reactor design and operation, essential for scaling up to industrial levels. EF reactor design encompasses factors affecting reaction kinetics, thermodynamics, and mass transfer, ultimately influencing DW treatment efficiency. These interconnected factors require thorough examination, with reactor simulation and statistical experimental design emerging as valuable tools for assessing the effects and interactions of operating variables in the EF degradation processes. In the case of the PEF reactor setup, it is crucial to factor in energy consumption to accurately evaluate the economic viability of the treatment process. Recently, more attention has been given to this significant aspect. While in certain instances, energy consumption might exceed that of EF process alone, the mineralization of contaminants achieved by the PEF process tends to be greater. For the SPEF approach, there is a need to develop photoreactors capable of treating significant volumes of DW by employing inexpensive materials and harnessing sunlight for irradiation. Considering the numerous factors involved in designing SPEF reactors, it is evident that the initial investment cost for this treatment approach is considerable. However, this expense is offset by the eco-friendly nature of the processes and by factoring in the low cost of solar energy. Thus, in certain regions, and for specific applications, the SPEF systems hold significant and promising potential for technological development. Further studies need to assess the techno-economic feasibility of different EAOPs reactors for scaling up based on the energy consumption and process output.

4. Operational Parameters Influencing EAOPs

4.1. Current Density

The current density regulates the production of $^\bullet OH$ radicals and different chlorinated species (Equations (21) and (22)). It also controls generation of H_2O_2 (Equation (9)), which determines the concentration of $^\bullet OH$ radicals in the wastewater solution for EF, PEF, and SPEF methods [41].

$$2Cl^- \rightarrow Cl_2 + 2e^- \tag{21}$$

$$Cl_2 + H_2O \rightarrow HClO + H^+ + Cl^- \tag{22}$$
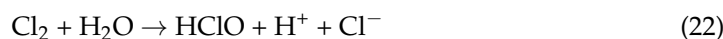
In general, increasing current density leads to a higher rate of pollutant degradation in EAOPs, as more oxidizing compounds are generated within a specific period [131,132]. Nevertheless, there is a limit to how much current density can be increased, as it also promotes parasitic reactions [38]. This results in a decrease in efficacy of energy and comparable to a smaller extent of pollutant removal compared to lower current densities. The parasitic reactions encompass various processes, including the formation of H_2O_2 through the dimerization of $M(^\bullet OH)$ (Equation (7)), the anodic oxidation of $M(^\bullet OH)$ leading to oxygen (Equation (6)), the coupling of $^\bullet OH$ resulting in H_2O_2, the electrochemical reduction in H_2O_2 (Equation (9)), the electrochemical oxidation of H_2O_2, the reaction of H_2O_2 with Fe^{3+} (Equation (12)), and the degradation of $^\bullet OH$ by the presence of H_2O_2 and Fe^{2+} (Equations (9)–(11)), respectively. These parasitic reactions have been discussed in previous research [47,133].

When choosing the most suitable current density, it is crucial to take into account both the degradation efficiency and current efficiency. Current efficiency pertains to the

practicality of EAOPs concerning the consumed electrical charge and energy consumption, especially in the context of large-scale electrochemical treatment systems. The mineralization current efficiency (MCE), expressed as a percentage, is a commonly used parameter to assess current efficiency. The MCE can be computed using Equation (23) [134].

$$\text{MCE} = \frac{n \, F \, V_s \, \Delta(DOC)_{exp}}{4.32 \times 10^7 \, m \, I \, t} \times 100 \tag{23}$$

In this equation, n corresponds to the number of electrons engaged in the mineralization process, F stands for Faraday's constant (96,485 C/mol), V_s indicates the volume of wastewater (liters), $\Delta(DOC)_{exp}$ signifies the reduction in dissolved organic carbon (mg/L), 4.32×10^7 refers to the conversion factor utilized for unit standardization (3600 s/h $\times$ 12,000 mg/mol), m represents the count of carbon particles in the studied compound, I symbolizes the current applied (amperes), and t denotes the treatment time (hours).

The specific energy consumption for operating the reactor per unit mass of total organic carbon (*SEC*, in kWh/g TOC) and per unit volume (*EC*, in kWh/m^3) might be computed by using Equations (24) and (25), respectively [135].

$$SEC = \frac{EIt}{V \, (C_o - C_t)} \tag{24}$$

$$EC = \frac{EIt}{V} \tag{25}$$

where E represents the average applied voltage (volts), I signifies applied current (amperes), t denotes the treatment time (hours), V denotes the volume of wastewater (liters), and C_o and C_t are the initial and final concentration of total organic carbon (mg/L), respectively. *SEC/EC* of different EAOPs are presented in Tables 1 and 2. In general, an elevated current density brings about lower MCE and higher *SEC* and/or *EC* [136].

The conductivity of the wastewater plays a crucial role in facilitating current density. Higher conductivity levels can enhance the efficiency of electrochemical treatments by promoting better ion transport and reaction kinetics. However, excessively high conductivity levels may require adjustments in process parameters to prevent electrode fouling or excessive energy consumption. Therefore, understanding the conductivity of the wastewater is essential for optimizing the performance of EAOPs for DW treatment.

In the EF process, increasing the current density in the reaction environment can boost the availability of electrons for the regeneration of Fe^{2+}, leading to the generation of more H_2O_2 molecules (Equation (9)). Consequently, this can lead to the generation of additional $^\bullet$OH on the electrodes. However, from both operational and economic perspectives, the rapid deterioration and frequent replacement of the anode are undesirable. Therefore, excessively high current densities are not recommended for DW treatment. Further studies can be conducted to assess the optimal current density to reduce the SEC or EC, which is related to the treatment cost.

4.2. pH

The EAOPs are highly influenced by pH. Previous studies on EF technology have consistently reported an optimal pH of around 3 [66,137,138]. At higher pH values, iron species in the EF process tend to precipitate as ferric hydroxides, reducing the reactivity of the Fenton reagent. Additionally, higher pH creates an alkaline environment that accelerates the decomposition of H_2O_2. Conversely, iron species form stable complexes with the oxidant H_2O_2, resulting in the deactivation of catalysts in acidic conditions. This significantly decreases the degradation efficiency of organic contaminants in DW. Zakeri et al. [122] studied COD removal from DW by applying electro-Fenton processes featuring different pH values at 3, 5 and 7. They observed the highest COD elimination rates of 90.3% after 60 min of treatment time with an applied voltage of 20V at pH 3 of initial wastewater

condition. They also found that the inclined pH condition decreased the generation of $^{\bullet}$OH compounds, which dropped down the degradation rate of COD in the EF process.

When employing AO treatment, the impact of pH is highly influenced by the characteristics of the organic contaminants present in the DW and the supporting electrolyte utilized during the electrolysis process. The impact of pH for the degradation of contaminants of DW was investigated across wide ranges of pH, signifying acidic and basic conditions [121]. It was found that the efficiency of pollutant removal exhibited a good performance at pH 7 or above [90,96,98]. This can be described as the thorough oxidation and/or chemical alteration of the surface of electrodes, specifically the anode. The study of pH impact on the removal efficiency of specific water pollutants is crucial, as pH values can vary in DW.

Based on previous research, lower pH is crucial for the EF, PEF, and SPEF approaches, whereas the AO process requires a higher pH (Tables 1 and 2). Most studies identified the optimal pH for EF, PEF, and SPEF processes as 3. In the AO process, the optimal pH varies above 7. In DW treatment, pH is an important factor for removing and recovering nutrients by applying EAOPs. Different concentrations of acid and alkaline solutions are used to decrease or increase the pH of DW, which increases operating costs. However, it is preferable to the determine optimum pH level of each treatment process to achieve maximum pollutant removal efficiency.

4.3. Hydrogen Peroxide Concentration

In the EF, PEF, and SPEF treatment, processes H_2O_2 is employed as an electro-generated oxidant at the cathode for the treatment of DW. Different carbonaceous cathodes are utilized to generate H_2O_2 by applying air or pure O_2 in the wastewater solution [38,44]. Cathodes with a high surface area, characterized by a porous structure, facilitate the electro-generation of H_2O_2 by supporting gas mass transport [139–141]. Rêgo et al. [142] studied several pieces of research to assess the presence of an electro-generated H_2O_2 concentration at different current densities and treatment times. Trigueros et al. [120] applied H_2O_2 in combination with the EC photochemical oxidation process for the treatment of DW. They observed 92.2% COD and 89.9% TOC for 14,000 mgL^{-1} H_2O_2 application along with UV/Fe^{2+}. Gong et al. [143] investigated the degradation of pollutants in the EF process to enhance biodegradability, utilizing carbon fiber felt as the cathode. They observed a quick pollutant removal by increasing current density from 2.22 to 6.67 mA cm^{-2}, which indicated an enhanced electro generation of $\bullet$OH radicals due to the availability of a high H_2O_2 concentration. Moreover, the decline in pollutants became more noticeable with a subsequent rise in current density to 6.67 mA cm^{-2}. This was due to the breakdown of H_2O_2 into O_2, taking place either on the anode surface or in the aqueous solution. Additionally, intermediate $HO_2^{\bullet}$ radicals were formed through the AO process [144].

In novel EAOPs, H_2O_2 is produced by the reduction in O_2 on the carbonaceous cathode surface. From a thermodynamic perspective, H_2O_2 is considered to be less potent than O_2. However, in terms of kinetics, particularly at ambient temperatures, H_2O_2 exhibits much greater efficiency. This implies that one strategy to improve the effectiveness of EAOPs involves promoting the generation of H_2O_2 through a reaction that would otherwise be unproductive at the cathode. The generation of H_2O_2 through the reduction in O_2 typically occurs across most cathode materials. However, for increasing efficiency, it is necessary to create a specific condition where the cathode, wastewater, and oxygen can interact. Consequently, a specialized type of porous cathode known as a gas diffusion cathode is utilized for this purpose. These cathodes facilitate the efficient formation of H_2O_2 by providing the necessary contact points between the cathode material, wastewater, and oxygen, thereby optimizing the performance of EAOPs.

4.4. Treatment Time

In EAOPs, various treatment times have been deployed (Tables 1 and 2). Ghazouani et al. [92] applied 357 A/m^2 current density for 6 h to obtain 88% COD removal by using BDD electrodes in the AO process for DW treatment. Ozturk and Yilmaz [99] obtained

93.5% TN removal and 99.9% color removal for 4 h of electrolysis time in the AO process for DW treatment. It was evident that, in the EF process, O_2 was continuously injected into the DW sample, resulting in the constant production of H_2O_2. Simultaneously, Fe^{2+} ions were generated on the surface of the cathode by the process of electrochemical reduction in Fe^{3+} ions [44]. Zakeri et al. [122] increased the efficiency of pollutant removal from 32% to 90% by increasing treatment time from 5 min to 120 min by applying the EF process for DW treatment. However, the improvement became marginal thereafter, reaching a saturation level after 60 min. This could be attributed to a decrease in the accessibility of ferrous ions caused by competing reactions, which was supported by the observation of a dark brown color in the DW sample due to the formation of iron-organic compounds [111]. Research has also documented an occurrence of equilibrium in pollutant removal that varies with time [25,121]. Hence, extended treatment time could enhance the efficacy of pollutant elimination in EAOP treatment until reaching a state of equilibrium.

4.5. Ferrous Ion Concentration

The Fe^{2+} ion plays a significant role in initiating the breakdown of H_2O_2 to form $^{\bullet}OH$ compounds in the Fenton reaction, as indicated by Equations (8)–(16). However, high concentrations of Fe^{2+} can impede the mechanism of mineralization by accelerating $^{\bullet}OH$ consumption [145]. To ensure effective control, it is necessary to properly manage the Fe^{2+} ion concentration. For organic pollutant degradation, the optimal Fe^{2+} ion concentration was determined to be 1 mM in the SPEF process [110]. In many cases, the H_2O_2/Fe^{2+} molar ratio has been used to investigate the EF approach for removing organic contaminants. For example, in the treatment of DW, increasing the molar ratio of H_2O_2/Fe^{2+} from 0.5 to 5.0 mL/L over a 90 min treatment period resulted in an increase in COD removal from 38% to 94%. This corresponds to higher amounts of H_2O_2 and Fe^{2+} in the solution [111]. However, it is important to note that the oxidation rate is significantly influenced by the Fe^{2+} concentration. For color removal, the degradation rate slightly increased with an increase in Fe^{2+} up to 0.2 mM, but remarkably decreased at Fe^{2+} concentrations above 0.3 mM [146]. By applying the SPEF process, the removal of organics from DW reached around 90% for 1 mM Fe^{2+} catalyst concentrations [110].

In EAOPs, Fe^{2+} plays a vital role in generating $\bullet OH$ radicals, which are highly reactive and effective in degrading organic pollutants. However, the effect of Fe^{2+} concentration is complex and requires careful management. A Fe^{2+} concentration that is too low may result in inadequate generation of $\bullet OH$ radicals, which leads to incomplete pollutant degradation. Conversely, excessively high Fe^{2+} concentrations can lead to faster $\bullet OH$ consumption and hinder the treatment process, thus reducing pollutant removal efficiency. The determination of the optimal Fe^{2+} concentration is important for potential treatment feasibility. In the PEF and SPEF processes, a 1 mM Fe^{2+} concentration exhibits good organic removal efficiency, but in the EF process, this concentration varies from 0.1 to 0.3 mM. However, it is necessary to determine an optimum concentration of Fe^{2+} in a pilot scale study to ensure efficient pollutant removal and to mitigate any adverse effects, such as excessive sludge formation or the generation of harmful by-products.

4.6. Electrode Selection

Selection of an appropriate electrode is a crucial factor in determining the performance of the EAOPs (Tables 1 and 2). In the EF process, a suitable cathode should possess high overvoltage for H_2 evolution, demonstrate outstanding stability and conductivity, and have minimal catalytic activity for H_2O_2 mineralization [147]. Similarly, ensuring the stability of anodes with a significant overpotential for O_2 evolution and consequent $^{\bullet}OH$ production is crucial for improving the EF method [148]. Electrodes exhibiting substantial overvoltage for O_2 can stimulate the production of $^{\bullet}OH$ radicals [149].

Platinum anodes have been extensively utilized to degrade various contaminants compared to other types of anodes. Pt exhibits high conductivity and stability, making it suitable for use in highly corrosive environments [54]. However, Pt electrodes have a

strong interaction with ●OH radicals, limiting their availability for contaminant degradation. Consequently, alternative materials, such as IrO_2/RuO_2-coated titanium and BDD electrodes, have been employed in the Fenton-based approaches. Among these materials, BDD electrodes have gained significant pollutant removal efficiency. Several studies have shown that BDD electrodes exhibit higher pollutants with lower energy consumption for DW treatment in comparison to other types of electrodes [88,107,116,117]. Additionally, the design of the reactor configuration plays a crucial role in ensuring effective current distribution for H_2O_2 accumulation and production [47].

In recent decades, there has been significant attention paid to graphite-based gas diffusion electrodes (GDEs) due to their ability to produce high amounts of H_2O_2. The porous structure of these electrodes facilitates the movement and internalization of O_2, leading to increased interfacial concentrations of O_2 and promoting greater H_2O_2 production. Various materials have been explored for GDE preparation, with carbon-PTFE, graphite-PTFE, etc. being particularly noteworthy for H_2O_2 production. For example, Zhang et al. [150] employed a GDE cathode to yield 60 mg/L of H_2O_2, which surpassed comparable GDEs solely relying on graphene. Utilizing a graphene-based GDE by applying a current density of 22 mA/cm^2 led to almost total elimination of pollutants. This implies that graphene boosts the permeability of the electroactive matrix, which elevates the density of the oxidative compounds for the degradation mechanisms. It also enhances electron transfer kinetics. The produced electrons can also engage in alternative reactions, like the synthesis of H_2O_2, through the interaction with O_2 evolution [151,152].

The mechanisms of carbonaceous electrode preparation may vary in different materials. Simple approaches like the heat treatment of carbon felt have been compared to more complex methods involving multi-step synthesis of graphene/graphite mixtures for GDE preparation [150,153]. Hence, the difficulty in this domain is creating pragmatic and uncomplicated synthesis approaches that yield consistent carbon structures with an elevated electrochemical performance for the generation of H_2O_2 compounds [154–156].

As an anode, Pt is widely used in EAOP treatment due to its high durability and conductivity characteristics. However, its strong interaction with OH● can impede the availability of oxidative radicals for pollutant removal from DW. Consequently, alternative materials, such as IrO_2/RuO_2-coated Ti and BDD, have been explored for this purpose. In recent times, BDD anodes have gained widespread adoption in EAOPs. The BDD electrode exhibits higher mineralization current efficiency and contaminant removal efficiency from DW in comparison to other materials. Furthermore, the selection of the electrodes plays a crucial role in enhancing the efficiency of current utilization for the generation and accumulation of H_2O_2 in EAOPs used for DW treatment.

4.7. Oxygen Flow Rate

For generating H_2O_2 electrochemically with carbonaceous electrodes, a continuous supply of oxygen is necessary [157]. This oxygen can be provided either through expensive pure oxygen or readily available air. Typically, elevated O_2 flow rates are employed alongside diverse carbonaceous cathodes to sustain O_2-saturated solutions, guaranteeing optimal electro generation of H_2O_2 [66,132]. Prior to electrolysis, oxygen gas is often introduced for a few minutes to saturate the aqueous solution. In the case of electrochemical cells with GDE, a balance must be struck between the flow rates of the liquid and O_2 to maintain comparable pressures on both surfaces of the cathode, preventing cell flooding [158,159]. Using a high flow rate of oxygen or compressed air can cause problems in EAOPs. The excessive amount of air or oxygen can reduce the interaction between wastewater and electrodes. Hence, improper interaction between electrodes and wastewater may hinder oxidative ion transfer during the electrolysis treatment of wastewater. Moreover, UV radiation exposure will be decreased in PEF and SPEF approaches. Due to these adverse effects, the proper flow rate of compressed air or O_2 should be maintained in the reactor [38,160]. According to Xia et al. [161], the optimal H_2O_2 dosage was attained with a 0.21 L/min O_2 flow rate. When the O_2 flow rate exceeded 0.28 Lmin^{-1}, an excessive generation of bubbles resulted

in a reduction in H_2O_2 production. It is crucial to highlight that the generation of H_2O_2 does not exhibit a linear increase with elevated O_2 flow rates. Once the oxygen saturation point is reached, further intensification of O_2 sparging does not significantly enhance the dissolved O_2 concentration or H_2O_2 generation [62,162]. The electrochemical generation of H_2O_2 maintains pollutant removal efficiency if it exceeds the oxygen saturation point. Consequently, before reaching the oxygen saturation point, the pollutant degradation increment will not be achieved.

4.8. Interelectrode Gap

The effectiveness of the EAOP is influenced by the distance between the electrodes, as it impacts the potential of the system and the energy consumption. In the context of treating DW, most of the reported research used interelectrode gaps of around 1 cm (Tables 1 and 2). A reduction in electrode distance leads to an increase in current flow and reduces resistivity obligation between anodes and cathodes [62]. Conversely, increasing the distance between electrodes prolongs the travel time of ions involved in the EAOPs, resulting in longer electrolysis times and a lower removal rate of pollutants [163]. The cathodic electro-regeneration of Fe^{2+} from Fe^{3+} is affected by the mass diffusion of Fe^{3+} at the point of contact between the cathode and the DW solution or the electron transfer between Fe^{3+} and the cathode [164]. Longer electrode distances limit the mass transformation of Fe^{3+} to the surface of cathode, hindering the regeneration of the catalyst and the performance of the EF process. Furthermore, increasing the electrode distance significantly increases energy consumption [122].

For EF process, interelectrode gap is very important (Table 2). A narrower gap between electrodes leads to decreased energy consumption and enhanced COD removal [149,165]. As an example, in the elimination of phenol with iron electrodes, there exists a clear correlation between interelectrode gap and process effectiveness. Optimal outcomes were obtained by incorporating activated carbon and maintaining an interelectrode gap of 4 cm, leading to a process efficiency of 75%. In a different study, a 5 cm interelectrode gap was maintained to remove 99% COD, 97% TN and 95% TP from DW by a combined electro-Fenton biological process [109].

From the findings, it can be said that the interelectrode gap significantly influences the efficiency of electrochemical DW treatment. A narrower gap enhances mass transfer rates and promotes uniform current distribution, potentially improving treatment efficiency. However, it also increases the risk of electrode fouling due to reduced space for contaminants to disperse. In contrast, a wider gap reduces fouling but may lead to uneven current distribution and higher energy consumption. Additionally, the gap size affects fluid dynamics within the treatment reactors, impacting mass transfer and overall treatment performance. Finding the optimal interelectrode gap involves balancing these factors to achieve effective pollutant removal while minimizing operational costs and energy consumption. Therefore, careful consideration of the interelectrode gap in terms of maximum pollutant removal and lower energy consumption must be taken into account in designing and optimizing EAOP treatment reactors for DW.

5. The Recovery of Value-Added Products from Dairy Wastewater

Value-added resource recovery from DW is essential for climate change mitigation and achieving environmental sustainability. In order to assess technological advancements in this field, it is necessary to consider the circular economy principles of reuse, recycling, and recovery of nutrients from DW [166]. Gallego-Schmid and Zepon-Tarpani [167] conducted a review of 43 research articles focusing on wastewater treatment management in developing countries using a life cycle assessment. Their results underscored the necessity for expanded research efforts to mitigate the environmental footprint, given that dairy wastewater contains valuable resources. Extracting nitrogen from these effluents using electrochemical systems, particularly through the recuperation of ammonia, has the potential to decrease energy consumption in the treatment of contaminated water [168]. Mohammed and

Ismail [169] attained complete nitrogen recovery efficiency through a nitrate influx rate of 0.011 kg-N m^3/day over a continuous operation period of 39 days, employing an integrated biological–electrochemical reactor. Ding et al. [89] recovered 65.1% phosphorous from DW by applying electrochemical treatment coupled with UASB system. They also found around 13% biogas generation increment as a by-product. Lee et al. [86] applied an electrochemical stripping process where they used platinum electrodes both as a cathode and anode and achieved 17,704 mg/L nitrogen recovery as ammonium sulfate fertilizer for 93.8 mA/cm^2 current density and 400 min electrolysis time. Xie and Popat [102] recovered up to 99.06% ammonia by utilizing a dual-chambered electrochemical ammonia stripping technique for DW. The recovered value-added products, which contain ample amounts of nutrients (nitrogen and phosphorus), can be used as an alternative source of chemical fertilizers. It also helps to mitigate greenhouse gas emissions to the environment from dairy farming systems [170,171]. Additionally, the environmental benefits of value-added product recovery must be carefully evaluated to ensure that the overall environmental footprint, including energy consumption, emissions, and resource utilization, is minimized and that potential trade-offs or unintended consequences are adequately addressed.

6. Hybrid Technology

Hybrid technologies refer to the integration of one or more conventional or advanced treatment methods to effectively eliminate contaminants. The reason for utilizing hybrid technologies is that no single treatment method can completely remove all compounds. This necessity arises due to the limitations of individual treatment technologies [172]. Various hybrid technologies have been employed to treat persistent pollutants from DW and decrease the overall treatment expenditure (Table 1). Turan [97] observed good results when he conducted a combined experiment for DW by applying an electro-oxidation (EO) process as a finishing technique after electrocoagulation, observing up to 98% turbidity removal efficiency. Li et al. [87] observed significant recovery of heavy metal when they applied an ultrasound-assisted AO hybrid technique for dairy wastewater treatment. This hybrid system reduces the treatment time. Alfonso-Muniozguren et al. [88] applied pre-ozonation as a pretreatment of slaughterhouse wastewater before applying EAOPs. They concluded that pre-ozonation increased the removal performance of EAOPs by converting organic pollutants into readily oxidizing components. Zakeri et al. [122] found tremendous results in removing pollutants from DW when they applied combined chemical coagulation with an EF hybrid system. Furthermore, Chakchouk et al. [96] conducted a comparison of how operating parameters affect the reduction in color, turbidity, and COD using EC, AO, and a combination of both techniques. Ultimately, the hybrid processes achieved complete removal of turbidity, a 90% reduction in color, and a 66.4% reduction in COD (Table 1) from DW. Similarly, the study examined the impact of varying current density on pollutant removal. The findings revealed that higher current density resulted in decreased levels of color, turbidity, and COD from DW. Incorporating electrochemical processes with other treatment technologies, whether used as an initial treatment approach or a final refining stage, has the potential to enhance its effectiveness and demonstrate the long-term viability of electrochemical treatment methods [109]. Indeed, the upcoming direction in this field should involve assessing the possibility of hybrid technologies to create cost-effective and efficient solutions capable of counteracting the adverse effect on the environment created by DW.

Several combined studies have employed EAOPs with other biological approaches. Vidal et al. [116] initially employed a comprehensive method that incorporated anaerobic digestion coupled with various advanced treatment approaches. These EAOPs encompassed AO, EF, and SPEF treatment techniques. The anaerobic digestion phase achieved a 90% reduction in COD, starting with about 1500 mg/L COD concentration, and generated around 90 mL of methane gas in 30 days of hydraulic residence time. The integrated approach elevated COD elimination by up to 97%, and the SPEF approach led to nearly complete mineralization of the pollutants. In a similar vein, Brooms et al. [173] investigated the

utilization of the biodegradability enhancement benefits of advanced oxidation processes through photodegradation. They integrated anaerobic digestion with photodegradation. The wastewater, identified as slaughterhouse wastewater, underwent anaerobic digestion as the primary treatment to eliminate fat, oil, and grease, as well as to generate energy for the following photochemical decomposition phase. The photodegradation process effectively eliminated persistent pollutants such as *O*-cresol and dibutyl phthalate while also increasing the biodegradability of the outflow from the anaerobic digester. The generated strong oxidizing agents during EAOPs can break down the organic components and stabilize the emulsions by reducing organic load and other contaminants, hence, improving the quality of treated wastewater.

Bustillo-Lecompte et al. [174] investigated the application of combined biological and EAOPs and conducted several research investigations involving photodegradation with H_2O_2 and UV photolysis along with anaerobic digestion. In a different investigation, a hybrid method was investigated, a sequence involving an anaerobic baffled reactor succeeded by a conventional activated sludge system, to eliminate organic pollutants [175].

Heidari et al. [109] carried out an investigation on the purification of DW by coupling EF with a sequencing batch reactor biological treatment approach. In this combined process, EF was applied to remove biodegradable compounds by generating oxidizing agents, which increased the intervention outcomes of the biological process. Ding et al. [89] applied UASB-integrated EAOPs to recover phosphate and enhance the biogas generation from DW. They recovered 68% phosphorous and found that EAOPs was a very effective treatment approach. To further eliminate organic substances and nutrients, the EF process was employed as a polishing approach. Under optimal conditions (pH 3, H_2O_2 1000 mg/L, Fe^{2+} 400 mg/L), COD and phosphate removal efficiency were achieved at 95.41% and 85.29%, respectively. The integration of both biological and EF methods resulted in the removal of 98.6% of COD and 90.5% of phosphate, highlighting the crucial role of the EF approach in effectively removing contaminants from DW [176]. Regarding the mentioned treatments, it was concluded that the potential to utilize integrated processes and determine the most effective approach is not only driven by enhanced pollutant removal efficiencies and cost savings but also by the mitigation of drawbacks associated with the processes and the elimination of potentially more toxic by-products generated during DW treatment. It is noteworthy that employing EAOPs either as a pretreatment or post-treatment step to biological processes is the most commonly employed technique for DW treatment [89,109,116].

Considering the advantageous characteristics and the synergistic benefits derived from combining various treatment techniques, employing integrated systems for DW treatment offers distinct advantages. Such treatment methodologies typically incorporate both electrochemical and biological approaches, either as a preliminary treatment or as a final refining step, depending on the specific objectives of the degradation process. These objectives may include overall pollutant removal or the targeted elimination of some pollutants. The primary objective of electrochemical pretreatment often involves partially oxidizing biologically resistant organic substances to generate less persistent intermediates. However, in the case of DW, a different approach has been adopted. Initially, the highly biodegradable fraction of DW is removed through anaerobic digestion, followed by the degradation of remaining recalcitrant contaminants via the electrochemical treatment process. This approach offers the advantage of utilizing biogas produced during anaerobic digestion to fulfill the energy requirements of the electrochemical process, thereby achieving cost reduction goals.

Therefore, the crucial aspect in combined approaches lies in optimizing process design. Pilot-scale investigations are essential for evaluating the advantages and limitations of the integrated systems in terms of economic viability, technical feasibility, and environmental impact. Indeed, the future direction in this field should focus on assessing the practicality of merging innovative and conventional technologies to develop cost-effective and efficient solutions capable of mitigating the adverse economic impact associated with DW.

7. Conclusions and Future Prospectives

Over the last several years, electrochemical technologies have emerged as a viable option for treating highly polluted DW. Electrochemical methods surpass biological treatment approaches in efficacy and reaction speed considering environmental friendliness and straightforwardness. At present time, EAOPs offer a particularly appealing approach for tackling emerging pollutants as these processes generate potent non-selective oxidants that are effective even at a high concentration of contaminants in DW.

The variation in degradation efficiency can be attributed to the different types of oxidizing agents produced in a specific approach and their ability to degrade pollutants within the system. In the AO process, oxidizing ●OH radicals are generated on the surface of the electrodes, which is influenced by several factors, such as the electrode material and applied current density. Conversely, the EF procedure entails the involvement of Fe^{2+}, encouraging the generation of oxygen-rich oxidizing components on both surfaces of electrodes and within the DW solution. The degradation mechanism is directly influenced by factors like Fe^{2+}, pH, and applied current density. The PEF and SPEF approaches take advantage of UV light, which generates an increased quantity of oxidizing components and enables faster degradation of pollutants from DW. Several factors influence the generation of oxidizing components in the PEF and SPEF approaches. Consequently, complex reactor design and chemicals are required for photo-assisted EAOPs, while AO processes are effective in a simple reactor design and chemical molecules. Integrated EAOPs with other technology can increase the performance of DW treatment. An intriguing but complex future endeavor involves assessing the economic viability of EAOPs for DW treatment. The evaluation must consider the installation cost of the reactor and operational expenses during the treatment performance. In the SPEF process, natural sunlight reduces energy cost and lowers total operational costs in comparison to the artificial PEF process. In contrast, the SPEF process can be hampered in cloudy weather conditions. Researchers have primarily focused on using EAOPs to treat DW on a laboratory scale. However, there is a need to scale up EAOPs for large-scale applications and industrial implementations.

Author Contributions: Conceptualization, methodology, validation, writing—original draft preparation, A.K.D.; writing—review and editing, supervision, funding acquisition, L.C. All authors have read and agreed to the published version of the manuscript.

Data Availability Statement: No new data were created or analyzed in this study. Data sharing is not applicable to this article.

Conflicts of Interest: The authors declare no conflicts of interest. The funders had no role in the design of the study; in the collection, analyses, or interpretation of data; in the writing of the manuscript; or in the decision to publish the results.

References

1. Burke, N.; Zacharski, K.A.; Southern, M.; Hogan, P.; Ryan, M.P.; Adley, C.C. The dairy industry: Process, monitoring, standards, and quality. *Des. Food Sci.* **2018**, *162*, 33–45. [CrossRef]
2. Owusu-Apenten, R.; Vieira, E. Dairy Products. In *Elementary Food Science*; Springer International Publishing: Cham, Switzerland, 2022; pp. 399–431. [CrossRef]
3. Dongre, A.; Sogani, M.; Sonu, K.; Syed, Z.; Sharma, G. Treatment of dairy wastewaters: Evaluating microbial fuel cell tools and mechanism. In *Environmental Issues and Sustainable Development*; IntechOpen: Rijeka, Croatia, 2020.
4. Das, A.K.; Reza, A.; Chen, L. Optimization of pollutants removal from anaerobically digested dairy wastewater by electro-oxidation process: A response surface methodology modeling and validation. *J. Appl. Electrochem.* **2024**, 1–22. [CrossRef]
5. Jindal, T.; Sinha, S.; Srivastava, A.; Mehrotra, T.; Singh, R. A review on the dairy industry waste water characteristics, its impact on environment and treatment possibilities. In *Emerging Issues in Ecology and Environmental Science: Case Studies from India*; Springer: Cham, Switzerland, 2019; pp. 73–84. [CrossRef]
6. Sutar, A.S.; Mulla, R.K.; Ranveer, A.C. Effluent treatment plant of dairy wastewater: A performance evaluation. *Int. Res. J. Eng. Technol.* **2015**, *2*, 837–840.

7. Shete, B.S.; Shinkar, N.P. Dairy industry wastewater sources, characteristics & its effects on environment. *Int. J. Curr. Eng. Technol.* **2013**, *3*, 1611–1615. Available online: http://inpressco.com/category/ijcet (accessed on 5 February 2024).

8. Yaqub, M.; Lee, W. Zero-liquid discharge (ZLD) technology for resource recovery from wastewater: A review. *Sci. Total. Environ.* **2019**, *681*, 551–563. [CrossRef]

9. Panagopoulos, A. Brine management (saline water & wastewater effluents): Sustainable utilization and resource recovery strategy through Minimal and Zero Liquid Discharge (MLD & ZLD) desalination systems. *Chem. Eng. Process.* **2022**, *176*, 108944. [CrossRef]

10. Ricky, R.; Shanthakumar, S.; Ganapathy, G.P.; Chiampo, F. Zero Liquid Discharge System for the Tannery Industry—An Overview of Sustainable Approaches. *Recycling* **2022**, *7*, 31. [CrossRef]

11. Gogoi, A.; Mazumder, P.; Tyagi, V.K.; Chaminda, G.T.; An, A.K.; Kumar, M. Occurrence and fate of emerging contaminants in water environment: A review. *Groundw. Sustain. Dev.* **2018**, *6*, 169–180. [CrossRef]

12. Pal, A.; Gin, K.Y.H.; Lin, A.Y.C.; Reinhard, M. Impacts of emerging organic contaminants on freshwater resources: Review of recent occurrences, sources, fate and effects. *Sci. Total Environ.* **2010**, *408*, 6062–6069. [CrossRef]

13. Goli, A.; Shamiri, A.; Khosroyar, S.; Talaiekhozani, A.; Sanaye, R.; Azizi, K. A review on different aerobic and anaerobic treatment methods in dairy industry wastewater. *J. Environ. Treat. Tech.* **2019**, *7*, 113–141. Available online: https://ssrn.com/abstract=3984721 (accessed on 5 February 2024).

14. Ganta, A.; Bashir, Y.; Das, S. Dairy Wastewater as a Potential Feedstock for Valuable Production with Concurrent Wastewater Treatment through Microbial Electrochemical Technologies. *Energies* **2022**, *15*, 9084. [CrossRef]

15. Obaideen, K.; Abdelkareem, M.A.; Wilberforce, T.; Elsaid, K.; Sayed, E.T.; Maghrabie, H.M.; Olabi, A.G. Biogas role in achievement of the sustainable development goals: Evaluation, Challenges, and Guidelines. *J. Taiwan Inst. Chem. Eng.* **2022**, *131*, 104207. [CrossRef]

16. Wang, G.; Côté, R. Integrating eco-efficiency and eco-effectiveness into the design of sustainable industrial systems in China. *Int. J. Sustain. Dev. World Ecol.* **2011**, *18*, 65–77. [CrossRef]

17. Yonar, T.; Sivrioğlu, Ö.; Özengin, N. Physico-chemical treatment of dairy industry wastewaters: A review. In *Technological Approaches for Novel Applications in Dairy Processing*; Intech: Nappanee, Indiana, 2018; Volume 179. [CrossRef]

18. Asghar, S.; Chen, L.; He, B.B. Optimization of Simultaneous Nutrients and Chemical Oxygen Demand Removal from Anaerobically Digested Liquid Dairy Manure in a Two-Step Fed Sequencing Batch Reactor System Using Taguchi Method and Grey Relational Analysis. *Appl. Biochem. Biotechnol.* **2023**, *196*, 537–557. [CrossRef]

19. Reig, M.; Vecino, X.; Cortina, J.L. Use of membrane technologies in dairy industry: An overview. *Foods* **2021**, *10*, 2768. [CrossRef]

20. Mateus, G.A.P.; Formentini-Schmitt, D.M.; Nishi, L.; Fagundes-Klen, M.R.; Gomes, R.G.; Bergamasco, R. Coagulation/flocculation with Moringa oleifera and membrane filtration for dairy wastewater treatment. *Water Air Soil Pollut.* **2017**, *228*, 342. [CrossRef]

21. Boavida-Dias, R.; Silva, J.R.; Santos, A.D.; Martins, R.C.; Castro, L.M.; Quinta-Ferreira, R.M. A Comparison of Biosolids Production and System Efficiency between Activated Sludge, Moving Bed Biofilm Reactor, and Sequencing Batch Moving Bed Biofilm Reactor in the Dairy Wastewater Treatment. *Sustainability* **2022**, *14*, 2702. [CrossRef]

22. Joshiba, G.J.; Kumar, P.S.; Femina, C.C.; Jayashree, E.; Racchana, R.; Sivanesan, S. Critical review on biological treatment strategies of dairy wastewater. *Desalin. Water Treat.* **2019**, *160*, 94–109. [CrossRef]

23. Todd, R.W.; Cole, N.A.; Casey, K.D.; Hagevoort, R.; Auvermann, B.W. Methane emissions from southern High Plains dairy wastewater lagoons in the summer. *Anim. Feed Sci. Technol.* **2011**, *166*, 575–580. [CrossRef]

24. Neczaj, E.; Kacprzak, M.; Kamizela, T.; Lach, J.; Okoniewska, E. Sequencing batch reactor system for the co-treatment of landfill leachate and dairy wastewater. *Desalination* **2008**, *222*, 404–409. [CrossRef]

25. Kushwaha, J.P.; Srivastava, V.C.; Mall, I.D. Sequential batch reactor for dairy wastewater treatment: Parametric optimization; kinetics and waste sludge disposal. *J. Environ. Chem. Eng.* **2013**, *1*, 1036–1043. [CrossRef]

26. Tawfik, A.; Sobhey, M.; Badawy, M. Treatment of a combined dairy and domestic wastewater in an up-flow anaerobic sludge blanket (UASB) reactor followed by activated sludge (AS system). *Desalination* **2008**, *227*, 167–177. [CrossRef]

27. Singh, K.; Arora, S. Removal of synthetic textile dyes from wastewaters: A critical review on present treatment technologies. *Crit. Rev. Environ. Sci. Technol.* **2011**, *41*, 807–878. [CrossRef]

28. Mo, W.; Zhang, Q. Energy–nutrients–water nexus: Integrated resource recovery in municipal wastewater treatment plants. *J. Environ. Manag.* **2013**, *127*, 255–267. [CrossRef]

29. Tyagi, V.K.; Lo, S.L. Sludge: A waste or renewable source for energy and resources recovery? *Ren. Sustain. Energy Rev.* **2013**, *25*, 708–728. [CrossRef]

30. Oturan, M.A.; Aaron, J.J. Advanced oxidation processes in water/wastewater treatment: Principles and applications. A review. *Crit. Rev. Environ. Sci. Technol.* **2014**, *44*, 2577–2641. [CrossRef]

31. Wang, J.L.; Xu, L.J. Advanced oxidation processes for wastewater treatment: Formation of hydroxyl radical and application. *Crit. Rev. Environ. Sci. Technol.* **2012**, *42*, 251–325. [CrossRef]

32. Tufail, A.; Price, W.E.; Mohseni, M.; Pramanik, B.K.; Hai, F.I. A critical review of advanced oxidation processes for emerging trace organic contaminant degradation: Mechanisms, factors, degradation products, and effluent toxicity. *J. Water Process Eng.* **2021**, *40*, 101778. [CrossRef]

33. Deng, Y.; Zhao, R. Advanced oxidation processes (AOPs) in wastewater treatment. *Curr. Pollut. Rep.* **2015**, *1*, 167–176. [CrossRef]

34. Ganiyu, S.O.; Oturan, N.; Raffy, S.; Esposito, G.; Van Hullebusch, E.D.; Cretin, M.; Oturan, M.A. Use of sub-stoichiometric titanium oxide as a ceramic electrode in anodic oxidation and electro-Fenton degradation of the beta-blocker propranolol: Degradation kinetics and mineralization pathway. *Electrochim. Acta* **2017**, *242*, 344–354. [CrossRef]

35. Marin, M.L.; Santos-Juanes, L.; Arques, A.; Amat, A.M.; Miranda, M.A. Organic photocatalysts for the oxidation of pollutants and model compounds. *Chem. Rev.* **2012**, *112*, 1710–1750. [CrossRef] [PubMed]

36. Gligorovski, S.; Strekowski, R.; Barbati, S.; Vione, D. Environmental implications of hydroxyl radicals (● OH). *Chem. Rev.* **2015**, *115*, 13051–13092. [CrossRef]

37. da Costa Moreira, M.F. Electrochemical Advanced Oxidation Processes: Application to the Degradation of Synthetic and Real Wastewaters. Ph.D. Thesis, University of Barcelona, Barcelona, Spain, 2016.

38. Moreira, F.C.; Boaventura, R.A.; Brillas, E.; Vilar, V.J. Electrochemical advanced oxidation processes: A review on their application to synthetic and real wastewaters. *Appl. Catal. B* **2017**, *202*, 217–261. [CrossRef]

39. Martínez-Huitle, C.A.; Panizza, M. Electrochemical oxidation of organic pollutants for wastewater treatment. *Curr. Opin. Electrochem.* **2018**, *11*, 62–71. [CrossRef]

40. Comninellis, C.; Kapalka, A.; Malato, S.; Parsons, S.A.; Poulios, I.; Mantzavinos, D. Advanced oxidation processes for water treatment: Advances and trends for R&D. *J. Chem. Technol. Biotechnol.* **2008**, *83*, 769–776. [CrossRef]

41. Brillas, E.; Sirés, I.; Oturan, M.A. Electro-Fenton process and related electrochemical technologies based on Fenton's reaction chemistry. *Chem. Rev.* **2009**, *109*, 6570–6631. [CrossRef] [PubMed]

42. Zhao, Q.; Zhao, X.; Cao, J. Advanced nanomaterials for degrading persistent organic pollutants. In *Advanced Nanomaterials for Pollutant Sensing and Environmental Catalysis*; Elsevier: Amsterdam, The Netherlands, 2020; pp. 249–305. [CrossRef]

43. Yang, N.; Yu, S.; Macpherson, J.V.; Einaga, Y.; Zhao, H.; Zhao, G.; Jiang, X. Conductive diamond: Synthesis, properties, and electrochemical applications. *Chem. Soc. Rev.* **2019**, *48*, 157–204. [CrossRef]

44. Brillas, E.; Garrido, J.A.; Rodríguez, R.M.; Arias, C.; Cabot, P.L.; Centellas, F. Wastewaters by Electrochemical Advanced Oxidation Processes Using a BDD Anode and Electrogenerated H~ 2O~ 2 with Fe (II) and UVA Light as Catalysts. *Port. Electrochim. Acta* **2008**, *26*, 15. [CrossRef]

45. Martínez-Huitle, C.A.; Brillas, E. Decontamination of wastewaters containing synthetic organic dyes by electrochemical methods: A general review. *Appl. Catal. B* **2009**, *87*, 105–145. [CrossRef]

46. Brillas, E.; Martínez-Huitle, C.A. Decontamination of wastewaters containing synthetic organic dyes by electrochemical methods. An updated review. *Appl. Catal. B* **2015**, *166*, 603–643. [CrossRef]

47. Sirés, I.; Brillas, E.; Oturan, M.A.; Rodrigo, M.A.; Panizza, M. Electrochemical advanced oxidation processes: Today and tomorrow. A review. *Environ. Sci. Pollut. Res.* **2014**, *21*, 8336–8367. [CrossRef] [PubMed]

48. Tchamango, S.; Nanseu-Njiki, C.P.; Ngameni, E.; Hadjiev, D.; Darchen, A. Treatment of dairy effluents by electrocoagulation using aluminium electrodes. *Sci. Total Environ.* **2010**, *408*, 947–952. [CrossRef] [PubMed]

49. Valente, G.F.S.; Santos Mendonça, R.C.; Pereira, J.A.M.; Felix, L.B. The efficiency of electrocoagulation in treating wastewater from a dairy industry, Part I: Iron electrodes. *J. Environ. Sci. Health* **2012**, *47*, 355–361. [CrossRef] [PubMed]

50. Şengil, İ.A. Treatment of dairy wastewaters by electrocoagulation using mild steel electrodes. *J. Hazard. Mat.* **2006**, *137*, 1197–1205. [CrossRef] [PubMed]

51. Bazrafshan, E.; Moein, H.; Kord Mostafapour, F.; Nakhaie, S. Application of electrocoagulation process for dairy wastewater treatment. *J. Chem.* **2013**, *2013*, 640139. [CrossRef]

52. Oturan, M.A.; Sirés, I.; Oturan, N.; Pérocheau, S.; Laborde, J.L.; Trévin, S. Sonoelectro-Fenton process: A novel hybrid technique for the destruction of organic pollutants in water. *J. Electroanal. Chem.* **2008**, *624*, 329–332. [CrossRef]

53. Barrera-Díaz, C.; Canizares, P.; Fernández, F.J.; Natividad, R.; Rodrigo, M.A. Electrochemical advanced oxidation processes: An overview of the current applications to actual industrial effluents. *J. Mex. Chem. Soc.* **2014**, *58*, 256–275. [CrossRef]

54. Panizza, M.; Cerisola, G. Direct and mediated anodic oxidation of organic pollutants. *Chem. Rev.* **2009**, *109*, 6541–6569. [CrossRef] [PubMed]

55. Ganzenko, O.; Huguenot, D.; Van Hullebusch, E.D.; Esposito, G.; Oturan, M.A. Electrochemical advanced oxidation and biological processes for wastewater treatment: A review of the combined approaches. *Environ. Sci. Pollut. Res.* **2014**, *21*, 8493–8524. [CrossRef]

56. Deng, Y.; Englehardt, J.D. Electrochemical oxidation for landfill leachate treatment. *Waste Manag.* **2007**, *27*, 380–388. [CrossRef]

57. Feng, L.; van Hullebusch, E.D.; Rodrigo, M.A.; Esposito, G.; Oturan, M.A. Removal of residual anti-inflammatory and analgesic pharmaceuticals from aqueous systems by electrochemical advanced oxidation processes. A review. *Chem. Eng. J.* **2013**, *228*, 944–964. [CrossRef]

58. Rodrigo, M.A.; Oturan, N.; Oturan, M.A. Electrochemically assisted remediation of pesticides in soils and water: A review. *Chem. Rev.* **2014**, *114*, 8720–8745. [CrossRef] [PubMed]

59. Martínez-Huitle, C.A.; Rodrigo, M.A.; Sirés, I.; Scialdone, O. Single and coupled electrochemical processes and reactors for the abatement of organic water pollutants: A critical review. *Chem. Rev.* **2015**, *115*, 13362–13407. [CrossRef] [PubMed]

60. Martínez-Sánchez, C.; Robles, I.; Godínez, L.A. Review of recent developments in electrochemical advanced oxidation processes: Application to remove dyes, pharmaceuticals, and pesticides. *Int. J. Environ. Sci. Technol.* **2022**, *19*, 12611–12678. [CrossRef]

61. Ghime, D.; Ghosh, P. Removal of organic compounds found in the wastewater through electrochemical advanced oxidation processes: A review. *Russ. J. Electrochem.* **2019**, *55*, 591–620. [CrossRef]

62. Shokri, A.; Nasernejad, B.; Sanavi Fard, M. Challenges and future roadmaps in heterogeneous electro-fenton process for wastewater treatment. *Wat. Air Soil Pollut.* **2023**, *34*, 153. [CrossRef] [PubMed]

63. Comninellis, C. Electrocatalysis in the electrochemical conversion/combustion of organic pollutants for wastewater treatment. *Electrochim. Acta* **1994**, *39*, 1857–1862.

64. Anglada, A.; Urtiaga, A.; Ortiz, I. Contributions of electrochemical oxidation to waste-water treatment: Fundamentals and review of applications. *J. Chem. Technol. Biotechnol.* **2009**, *84*, 1747–1755. [CrossRef]

65. Moreira, F.C.; Garcia-Segura, S.; Boaventura, R.A.; Brillas, E.; Vilar, V.J. Degradation of the antibiotic trimethoprim by electro-chemical advanced oxidation processes using a carbon-PTFE air-diffusion cathode and a boron-doped diamond or platinum anode. *Appl. Catal. B* **2014**, *160*, 492–505. [CrossRef]

66. Brillas, E. Recent development of electrochemical advanced oxidation of herbicides. A review on its application to wastewater treatment and soil remediation. *J. Clean. Prod.* **2021**, *290*, 125841. [CrossRef]

67. Martínez-Huitle, C.A.; Rodrigo, M.A.; Sirés, I.; Scialdone, O. A critical review on latest innovations and future challenges of electrochemical technology for the abatement of organics in water. *Appl. Catal. B* **2023**, *328*, 122430. [CrossRef]

68. Nidheesh, P.V.; Zhou, M.; Oturan, M.A. An overview on the removal of synthetic dyes from water by electrochemical advanced oxidation processes. *Chemosphere* **2018**, *197*, 210–227. [CrossRef] [PubMed]

69. Martinez-Huitle, C.A.; Ferro, S. Electrochemical oxidation of organic pollutants for the wastewater treatment: Direct and indirect processes. *Chem. Soc. Rev.* **2006**, *35*, 1324–1340. [CrossRef] [PubMed]

70. Poza-Nogueiras, V.; Rosales, E.; Pazos, M.; Sanroman, M.A. Current advances and trends in electro-Fenton process using heterogeneous catalysts—A review. *Chemosphere* **2018**, *201*, 399–416. [CrossRef] [PubMed]

71. Monteil, H.; Pechaud, Y.; Oturan, N.; Oturan, M.A. A review on efficiency and cost effectiveness of electro-and bio-electro-Fenton processes: Application to the treatment of pharmaceutical pollutants in water. *Chem. Eng. J.* **2019**, *376*, 119577. [CrossRef]

72. Otsuka, K.; Hosokawa, K.; Yamanaka, I.; Wada, Y.; Morikawa, A. One-step oxidation of benzene to phenol applying a fuel cell system. *Electrochim. Acta* **1989**, *34*, 1485–1488. [CrossRef]

73. Arnold, S.M.; Hickey, W.J.; Harris, R.F. Degradation of atrazine by Fenton's reagent: Condition optimization and product quantification. *Environ. Sci. Technol.* **1995**, *29*, 2083–2089. [CrossRef] [PubMed]

74. Brillas, E.; Mur, E.; Sauleda, R.; Sanchez, L.; Peral, J.; Domènech, X.; Casado, J. Aniline mineralization by AOP's: Anodic oxidation, photocatalysis, electro-Fenton and photoelectro-Fenton processes. *Appl. Catal. B* **1998**, *16*, 31–42. [CrossRef]

75. Brillas, E. A review on the degradation of organic pollutants in waters by UV photoelectro-Fenton and solar photoelectro-Fenton. *J. Braz. Chem. Soc.* **2014**, *25*, 393–417. [CrossRef]

76. Zhou, M.; Yu, Q.; Lei, L.; Barton, G. Electro-Fenton method for the removal of methyl red in an efficient electrochemical system. *Sep. Purif. Technol.* **2007**, *57*, 380–387. [CrossRef]

77. Peralta-Hernández, J.M.; Martínez-Huitle, C.A.; Guzmán-Mar, J.L.; Hernández-Ramírez, A. Recent advances in the application of electro-Fenton and photoelectro-Fenton process for removal of synthetic dyes in wastewater treatment. *J. Environ. Eng. Manag.* **2009**, *19*, 257–265.

78. Moreira, F.C.; Boaventura, R.A.; Brillas, E.; Vilar, V.J. Degradation of trimethoprim antibiotic by UVA photoelectro-Fenton process mediated by Fe (III)–carboxylate complexes. *Appl. Catal. B* **2015**, *162*, 34–44. [CrossRef]

79. Brillas, E. A review on the photoelectro-Fenton process as efficient electrochemical advanced oxidation for wastewater remediation. Treatment with UV light, sunlight, and coupling with conventional and other photo-assisted advanced technologies. *Chemosphere* **2020**, *250*, 126198. [CrossRef]

80. Borràs, N.; Arias, C.; Oliver, R.; Brillas, E. Anodic oxidation, electro-Fenton and photoelectro-Fenton degradation of cyanazine using a boron-doped diamond anode and an oxygen-diffusion cathode. *J. Electroanal. Chem.* **2013**, *689*, 158–167. [CrossRef]

81. Belle, U.; Invernizzi, M.; Polvara, E.; Lucotti, A.; Diamanti, M.V.; Sironi, S.; Pedeferri, M. A novel nanotubular TiO_2-based Plug-Flow reactor for gas phase photocatalytic degradation of toluene. *Chem. Eng. J.* **2022**, *437*, 135323. [CrossRef]

82. Cheng, M.; Zeng, G.; Huang, D.; Lai, C.; Xu, P.; Zhang, C.; Liu, Y. Hydroxyl radicals based advanced oxidation processes (AOPs) for remediation of soils contaminated with organic compounds: A review. *Chem. Eng. J.* **2016**, *284*, 582–598. [CrossRef]

83. Spasiano, D.; Marotta, R.; Malato, S.; Fernandez-Ibanez, P.; Di Somma, I. Solar photocatalysis: Materials, reactors, some commercial, and pre-industrialized applications. A comprehensive approach. *Appl. Catal. B* **2015**, *170*, 90–123. [CrossRef]

84. Liu, J.; Ren, N.; Qu, C.; Lu, S.; Xiang, Y.; Liang, D. Recent Advances in the Reactor Design for Industrial Wastewater Treatment by Electro-Oxidation Process. *Water* **2022**, *14*, 3711. [CrossRef]

85. Perry, S.C.; de León, C.P.; Walsh, F.C. The Design, Performance and Continuing Development of Electrochemical Reactors for Clean Electrosynthesis. *J. Electrochem. Soc.* **2020**, *167*, 155525. [CrossRef]

86. Lee, G.; Kim, K.; Chung, J.; Han, J.I. Electrochemical ammonia accumulation and recovery from ammonia-rich livestock wastewater. *Chemosphere* **2021**, *270*, 128631. [CrossRef]

87. Li, C.; Xue, B.; Wang, S.; Zhang, X.; Zhao, C.; Yang, X.; Wang, J. An Innovative Digestion Method: Ultrasound-Assisted Electrochemical Oxidation for the Onsite Extraction of Heavy Metal Elements in Dairy Farm Slurry. *Materials* **2021**, *14*, 4562. [CrossRef] [PubMed]

88. Alfonso-Muniozguren, P.; Cotillas, S.; Boaventura, R.A.; Moreira, F.C.; Lee, J.; Vilar, V.J. Single and combined electrochemical oxidation driven processes for the treatment of slaughterhouse wastewater. *J. Clean. Prod.* **2020**, *270*, 121858. [CrossRef]

89. Ding, L.; Lin, H.; Zamalloa, C.; Hu, B. Simultaneous phosphorus recovery, sulfide removal, and biogas production improvement in electrochemically assisted anaerobic digestion of dairy manure. *Sci. Total Environ.* **2021**, *777*, 146226. [CrossRef]

90. Markou, V.; Kontogianni, M.C.; Frontistis, Z.; Tekerlekopoulou, A.G.; Katsaounis, A.; Vayenas, D. Electrochemical treatment of biologically pre-treated dairy wastewater using dimensionally stable anodes. *J. Environ. Manag.* **2017**, *202*, 217–224. [CrossRef] [PubMed]

91. Lei, X.; Maekawa, T. Electrochemical treatment of anaerobic digestion effluent using a Ti/Pt–IrO$_2$ electrode. *Bioresour. Technol.* **2007**, *98*, 3521–3525. [CrossRef] [PubMed]

92. Ghazouani, M.; Akrout, H.; Jellali, S.; Bousselmi, L. Comparative study of electrochemical hybrid systems for the treatment of real wastewaters from agri-food activities. *Sci. Total Environ.* **2019**, *647*, 1651–1664. [CrossRef] [PubMed]

93. Abdelhay, A.; Jum'h, I.; Albsoul, A.; Al Tarazi, D. Dairy wastewater remediation using electrochemical oxidation on boron doped diamond anode (BDD). *Desalin. Water Treat.* **2019**, *171*, 177–182. [CrossRef]

94. Ghazouani, M.; Akrout, H.; Bousselmi, L. Nitrate and carbon matter removals from real effluents using Si/BDD electrode. *Environ. Sci. Pollut. Res.* **2017**, *24*, 9895–9906. [CrossRef] [PubMed]

95. Güven, G.; Perendeci, A.; Tanyolaç, A. Electrochemical treatment of deproteinated whey wastewater and optimization of treatment conditions with response surface methodology. *J. Hazard. Mat.* **2008**, *157*, 69–78. [CrossRef]

96. Chakchouk, I.; Elloumi, N.; Belaid, C.; Mseddi, S.; Chaari, L.; Kallel, M. A combined electrocoagulation-electrooxidation treatment for dairy wastewater. *Braz. J. Chem. Eng.* **2017**, *34*, 109–117. [CrossRef]

97. Turan, N.B. The application of hybrid electrocoagulation–electrooxidation system for the treatment of dairy wastewater using different electrode connections. *Sep. Sci. Technol.* **2021**, *56*, 1788–1801. [CrossRef]

98. de Sousa, D.D.P.; Pinto, C.F.; Tonhela, M.A.; Granato, A.C.; Motheo, A.D.J.; Lima, A.D.F.; Malpass, G.R.P. Treatment of real dairy wastewater by electrolysis and photo-assisted electrolysis in presence of chlorides. *Water Sci. Technol.* **2019**, *80*, 961–969. [CrossRef] [PubMed]

99. Ozturk, D.; Yilmaz, A.E. Treatment of slaughterhouse wastewater with the electrochemical oxidation process: Role of operating parameters on treatment efficiency and energy consumption. *J. Water Process Eng.* **2019**, *31*, 100834. [CrossRef]

100. Borbón, B.; Oropeza-Guzman, M.T.; Brillas, E.; Sirés, I. Sequential electrochemical treatment of dairy wastewater using aluminum and DSA-type anodes. *Environ. Sci. Pollut. Res.* **2014**, *21*, 8573–8584. [CrossRef]

101. Sandoval, M.A.; Espinoza, L.C.; Coreño, O.; García, V.; Fuentes, R.; Thiam, A.; Salazar, R. A comparative study of anodic oxidation and electrocoagulation for treating cattle slaughterhouse wastewater. *J. Environ. Chem. Eng.* **2022**, *10*, 108306. [CrossRef]

102. Xie, A.; Popat, S.C. Electrochemical ammonia stripping from non-nitrified animal rendering wastewater. *Chem. Eng. J. Adv.* **2020**, *3*, 100020. [CrossRef]

103. Tirado, L.; Gökkuş, Ö.; Brillas, E.; Sirés, I. Treatment of cheese whey wastewater by combined electrochemical processes. *J. Appl. Electrochem.* **2018**, *48*, 1307–1319. [CrossRef]

104. Stylianou, M.; Montel, E.; Dermentzis, K.; Agapiou, A. Electrochemical treatment of cattle wastewater samples. *Waste Biomass Valorization* **2020**, *11*, 5185–5196. [CrossRef]

105. Ihara, I.; Umetsu, K.; Kanamura, K.; Watanabe, T. Electrochemical oxidation of the effluent from anaerobic digestion of dairy manure. *Bioresour. Technol.* **2006**, *97*, 1360–1364. [CrossRef]

106. Won, S.G.; Jeon, D.Y.; Rahman, M.M.; Kwag, J.H.; Ra, C.S. Optimization of electrochemical reaction for nitrogen removal from biological secondary-treated milking center wastewater. *Environ. Technol.* **2016**, *37*, 1510–1519. [CrossRef]

107. Paramo-Vargas, J.; Camargo, A.M.E.; Gutierrez-Granados, S.; Godinez, L.A.; Peralta-Hernandez, J.M. Applying electro-Fenton process as an alternative to a slaughterhouse effluent treatment. *J. Electroanal. Chem.* **2015**, *754*, 80–86. [CrossRef]

108. Kuang, C.; Xu, Y.; Lai, W.; Xie, G.; Pan, Z.; Zheng, L.; Zhou, X. Novel electrodes for cathode electro-Fenton oxidation coupled with anodic oxidation system for advanced treatment of livestock wastewater. *Electrochim. Acta* **2019**, *321*, 134605. [CrossRef]

109. Heidari, M.R.; Malakootian, M.; Boczkaj, G.; Sun, X.; Tao, Y.; Sonawane, S.H.; Mehdizadeh, H. Evaluation and start-up of an electro-Fenton-sequencing batch reactor for dairy wastewater treatment. *Water Res. Ind.* **2021**, *25*, 100149. [CrossRef]

110. Vidal, J.; Carvajal, A.; Huilinir, C.; Salazar, R. Slaughterhouse wastewater treatment by a combined anaerobic digestion/solar photoelectro-Fenton process performed in semicontinuous operation. *Chem. Eng. J.* **2019**, *378*, 122097. [CrossRef]

111. Davarnejad, R.; Nikseresht, M. Dairy wastewater treatment using an electrochemical method: Experimental and statistical study. *J. Electroanal. Chem.* **2016**, *775*, 364–373. [CrossRef]

112. Davarnejad, R.; Nikseresht, M.; Ajideh, I. An efficient technique for dairy wastewater treatment. *Int. J. Dairy Technol.* **2018**, *71*, 532–538. [CrossRef]

113. Camcıoğlu, Ş.; Özyurt, B.; Şengül, S.; Hapoğlu, H. Evaluation of electro-Fenton method on cheese whey treatment: Optimization through response surface methodology. *Desalin. Water Treat.* **2019**, *172*, 270–280. [CrossRef]

114. Akkaya, G.K.; Erkan, H.S.; Sekman, E.; Top, S.; Karaman, H.; Bilgili, M.S.; Engin, G.O. Modeling and optimizing Fenton and electro-Fenton processes for dairy wastewater treatment using response surface methodology. *Int. J. Environ. Sci. Technol.* **2019**, *16*, 2343–2358. [CrossRef]

115. Thirugnanasambandham, K.; Ganesamoorthy, R. Dual treatment of milk processing industry wastewater using electro fenton process followed by anaerobic treatment. *Int. J. Chem. React. Eng.* **2019**, *17*, 20190074. [CrossRef]

116. Vidal, J.; Huiliñir, C.; Salazar, R. Removal of organic matter contained in slaughterhouse wastewater using a combination of anaerobic digestion and solar photoelectro-Fenton processes. *Electrochim. Acta* **2016**, *210*, 163–170. [CrossRef]

117. Feyzi, Z.; Samadian, M.; Nemati, B.; Faraji, H. Evaluation of the combined Anaerobic Digestion/Solar photoelectro-Fenton process: Removal of organic matter contained in slaughterhouse wastewater. *J. Water Process Eng.* **2022**, 1–18. Available online: https://ssrn.com/abstract=4183992 (accessed on 20 February 2024). [CrossRef]
118. Bruguera-Casamada, C.; Araujo, R.M.; Brillas, E.; Sires, I. Advantages of electro-Fenton over electrocoagulation for disinfection of dairy wastewater. *Chem. Eng. J.* **2019**, *376*, 119975. [CrossRef]
119. Páramo-Vargas, J.; Granados, S.G.; Maldonado-Rubio, M.I.; Peralta-Hernández, J.M. Up to 95% reduction of chemical oxygen demand of slaughterhouse effluents using Fenton and photo-Fenton oxidation. *Environ. Chem. Lett.* **2016**, *14*, 149–154. [CrossRef]
120. Trigueros, D.E.; Braun, L.; Hinterholz, C.L. Optimal electrocoagulation as a post-treatment to photochemical oxidation: Minimal electrical energy consumption and lower acute toxicity of dairy wastewater. *J. Photochem. Photobiol. A* **2023**, *437*, 114496. [CrossRef]
121. Kushwaha, J.P.; Srivastava, V.C.; Mall, I.D. Organics removal from dairy wastewater by electrochemical treatment and residue disposal. *Sep. Purif. Technol.* **2010**, *76*, 198–205. [CrossRef]
122. Zakeri, H.R.; Yousefi, M.; Mohammadi, A.A.; Baziar, M.; Mojiri, S.A.; Salehnia, S.; Hosseinzadeh, A. Chemical coagulation-electro fenton as a superior combination process for treatment of dairy wastewater: Performance and modelling. *Int. J. Environ. Sci. Technol.* **2021**, *18*, 3929–3942. [CrossRef]
123. Mohmmad, A.R.R.E.J.; Hamed Mosavian, M.T.; Haddad Khodaparast, M.H. Electro-Fenton technology for dairy wastewater treatment. *Int. J. Environ. Sci. Technol.* **2023**, *21*, 35–42. [CrossRef]
124. Yavuz, Y.; Öcal, E.; Koparal, A.S.; Öğütveren, Ü.B. Treatment of dairy industry wastewater by EC and EF processes using hybrid Fe-Al plate electrodes. *J. Chem. Technol. Biotechnol.* **2011**, *86*, 964–969. [CrossRef]
125. Bazrafshan, E.; Zakeri, H.R.; Vieira, M.G.A.; Derakhshan, Z.; Mohammadi, L.; Mohammadpour, A.; Mousavi Khaneghah, A. Slaughterhouse Wastewater Treatment by Integrated Chemical Coagulation and Electro-Fenton Processes. *Sustainability* **2022**, *14*, 11407. [CrossRef]
126. Samet, Y.; Agengui, L.; Abdelhédi, R. Electrochemical degradation of chlorpyrifos pesticide in aqueous solutions by anodic oxidation at boron-doped diamond electrodes. *Chem. Eng. J.* **2010**, *161*, 167–172. [CrossRef]
127. Frangos, P.; Shen, W.; Wang, H.; Li, X.; Yu, G.; Deng, S.; Wang, Y. Improvement of the degradation of pesticide deethylatrazine by combining UV photolysis with electrochemical generation of hydrogen peroxide. *Chem. Eng. J.* **2016**, *291*, 215–224. [CrossRef]
128. Radjenovic, J.; Sedlak, D.L. Challenges and opportunities for electrochemical processes as next-generation technologies for the treatment of contaminated water. *Environ. Sci. Technol.* **2015**, *49*, 11292–11302. [CrossRef] [PubMed]
129. Ghanbari, F.; Hassani, A.; Wacławek, S.; Wang, Z.; Matyszczak, G.; Lin, K.Y.A.; Dolatabadi, M. Insights into paracetamol degradation in aqueous solutions by ultrasound-assisted heterogeneous electro-Fenton process: Key operating parameters, mineralization and toxicity assessment. *Sep. Purif. Technol.* **2021**, *266*, 118533. [CrossRef]
130. Fatta-Kassinos, D.; Vasquez, M.I.; Kümmerer, K. Transformation products of pharmaceuticals in surface waters and wastewater formed during photolysis and advanced oxidation processes–degradation, elucidation of byproducts and assessment of their biological potency. *Chemosphere* **2011**, *85*, 693–709. [CrossRef] [PubMed]
131. Garcia-Segura, S.; Lima, Á.S.; Cavalcanti, E.B.; Brillas, E. Anodic oxidation, electro-Fenton and photoelectro-Fenton degradations of pyridinium-and imidazolium-based ionic liquids in waters using a BDD/air-diffusion cell. *Electrochim. Acta* **2016**, *198*, 268–279. [CrossRef]
132. Boye, B.; Dieng, M.M.; Brillas, E. Degradation of herbicide 4-chlorophenoxyacetic acid by advanced electrochemical oxidation methods. *Environ. Sci. Technol.* **2002**, *36*, 3030–3035. [CrossRef] [PubMed]
133. Marselli, B.; Garcia-Gomez, J.; Michaud, P.A.; Rodrigo, M.A.; Comninellis, C. Electrogeneration of hydroxyl radicals on boron-doped diamond electrodes. *J. Electrochem. Soc.* **2003**, *150*, D79. [CrossRef]
134. Skoumal, M.; Arias, C.; Cabot, P.L.; Centellas, F.; Garrido, J.A.; Rodríguez, R.M.; Brillas, E. Mineralization of the biocide chloroxylenol by electrochemical advanced oxidation processes. *Chemosphere* **2008**, *71*, 1718–1729. [CrossRef] [PubMed]
135. Flox, C.; Garrido, J.A.; Rodríguez, R.M.; Cabot, P.L.; Centellas, F.; Arias, C.; Brillas, E. Mineralization of herbicide mecoprop by photoelectro-Fenton with UVA and solar light. *Catal. Today* **2007**, *129*, 29–36. [CrossRef]
136. Ruiz, E.J.; Hernández-Ramírez, A.; Peralta-Hernández, J.M.; Arias, C.; Brillas, E. Application of solar photoelectro-Fenton technology to azo dyes mineralization: Effect of current density, Fe^{2+} and dye concentrations. *Chem. Eng. J.* **2011**, *171*, 385–392. [CrossRef]
137. Garcia-Segura, S.; Almeida, L.C.; Bocchi, N.; Brillas, E. Solar photoelectro-Fenton degradation of the herbicide 4-chloro-2-methylphenoxyacetic acid optimized by response surface methodology. *J. Hazard. Mater.* **2011**, *194*, 109–118. [CrossRef] [PubMed]
138. David, C.; Arivazhagan, M.; Tuvakara, F. Decolorization of distillery spent wash effluent by electro oxidation (EC and EF) and Fenton processes: A comparative study. *Ecotoxicol. Environ. Saf.* **2015**, *121*, 142–148. [CrossRef] [PubMed]
139. Çelebi, M.S.; Oturan, N.; Zazou, H.; Hamdani, M.; Oturan, M.A. Electrochemical oxidation of carbaryl on platinum and boron-doped diamond anodes using electro-Fenton technology. *Sep. Purif. Technol.* **2015**, *156*, 996–1002. [CrossRef]
140. Wang, Y.; Zhao, H.; Chai, S.; Wang, Y.; Zhao, G.; Li, D. Electrosorption enhanced electro-Fenton process for efficient mineralization of imidacloprid based on mixed-valence iron oxide composite cathode at neutral pH. *Chem. Eng. J.* **2013**, *223*, 524–535. [CrossRef]
141. Zhang, C.; Zhou, M.; Ren, G.; Yu, X.; Ma, L.; Yang, J.; Yu, F. Heterogeneous electro-Fenton using modified iron–carbon as catalyst for 2, 4-dichlorophenol degradation: Influence factors, mechanism and degradation pathway. *Water Res.* **2015**, *70*, 414–424. [CrossRef]

142. Rêgo, F.E.F.; Solano, A.M.S.; da Costa Soares, I.C.; da Silva, D.R.; Huitle, C.A.M.; Panizza, M. Application of electro-Fenton process as alternative for degradation of Novacron Blue dye. *J. Environ. Chem. Eng.* **2014**, *2*, 875–880. [CrossRef]

143. Gong, Y.; Li, J.; Zhang, Y.; Zhang, M.; Tian, X.; Wang, A. Partial degradation of levofloxacin for biodegradability improvement by electro-Fenton process using an activated carbon fiber felt cathode. *J. Hazard. Mat.* **2016**, *304*, 320–328. [CrossRef] [PubMed]

144. Kuznetsova, E.V.; Savinov, E.N.; Vostrikova, L.A.; Parmon, V.N. Heterogeneous catalysis in the Fenton-type system FeZSM-5/H_2O_2. *Appl. Catal. B* **2004**, *51*, 165–170. [CrossRef]

145. Wang, Y.; Liu, Y.; Wang, K.; Song, S.; Tsiakaras, P.; Liu, H. Preparation and characterization of a novel KOH activated graphite felt cathode for the electro-Fenton process. *Appl. Catal. B* **2015**, *165*, 360–368. [CrossRef]

146. Meijide, J.; Gómez, J.; Pazos, M.; Sanromán, M.A. Degradation of thiamethoxam by the synergetic effect between anodic oxidation and Fenton reactions. *J. Hazard. Mat.* **2016**, *319*, 43–50. [CrossRef]

147. Khataee, A.; Hasanzadeh, A. Modified cathodes with carbon-based nanomaterials for electro-Fenton process. In *Electro-Fenton Process: New Trends and Scale-Up*; Springer: Singapore, 2018; pp. 111–143. [CrossRef]

148. Sopaj, F.; Oturan, N.; Pinson, J.; Podvorica, F.; Oturan, M.A. Effect of the anode materials on the efficiency of the electro-Fenton process for the mineralization of the antibiotic sulfamethazine. *Appl. Catal. B* **2016**, *199*, 331–341. [CrossRef]

149. Marlina, E. Electro-Fenton for industrial wastewater treatment: A review. *E3S Web Conf.* **2019**, *125*, 03003. [CrossRef]

150. Zhang, Z.; Meng, H.; Wang, Y.; Shi, L.; Wang, X.; Chai, S. Fabrication of graphene@ graphite-based gas diffusion electrode for improving H_2O_2 generation in Electro-Fenton process. *Electrochim. Acta* **2018**, *260*, 112–120. [CrossRef]

151. Salmerón, I.; Oller, I.; Plakas, K.V.; Malato, S. Carbon-based cathodes degradation during electro-Fenton treatment at pilot scale: Changes in H_2O_2 electro generation. *Chemosphere* **2021**, *275*, 129962. [CrossRef] [PubMed]

152. Zhou, W.; Meng, X.; Rajic, L.; Xue, Y.; Chen, S.; Ding, Y.; Alshawabkeh, A.N. "Floating" cathode for efficient H_2O_2 electro-generation applied to degradation of ibuprofen as a model pollutant. *Electrochem. Commun.* **2018**, *96*, 37–41. [CrossRef] [PubMed]

153. Le, T.X.H.; Van Nguyen, T.; Yacouba, Z.A.; Zoungrana, L.; Avril, F.; Petit, E.; Cretin, M. Toxicity removal assessments related to degradation pathways of azo dyes: Toward an optimization of electro-Fenton treatment. *Chemosphere* **2016**, *161*, 308–318. [CrossRef] [PubMed]

154. Sun, Y.; Sinev, I.; Ju, W.; Bergmann, A.; Dresp, S.; Kühl, S.; Strasser, P. Efficient electrochemical hydrogen peroxide production from molecular oxygen on nitrogen-doped mesoporous carbon catalysts. *Acs Catal.* **2018**, *8*, 2844–2856. [CrossRef]

155. Zhou, W.; Rajic, L.; Chen, L.; Kou, K.; Ding, Y.; Meng, X.; Alshawabkeh, A.N. Activated carbon as effective cathode material in iron-free Electro-Fenton process: Integrated H_2O_2 electrogeneration, activation, and pollutants adsorption. *Electrochim. Act.* **2019**, *296*, 317–326. [CrossRef] [PubMed]

156. Miao, J.; Zhu, H.; Tang, Y.; Chen, Y.; Wan, P. Graphite felt electrochemically modified in H_2SO_4 solution used as a cathode to produce H2O2 for pre-oxidation of drinking water. *Chem. Eng. J.* **2014**, *250*, 312–318. [CrossRef]

157. Garcia-Rodriguez, O.; Mousset, E.; Olvera-Vargas, H.; Lefebvre, O. Electrochemical treatment of highly concentrated wastewater: A review of experimental and modeling approaches from lab-to full-scale. *Crit. Rev. Environ. Sci. Technol.* **2022**, *52*, 240–309. [CrossRef]

158. Labiadh, L.; Oturan, M.A.; Panizza, M.; Hamadi, N.B.; Ammar, S. Complete removal of AHPS synthetic dye from water using new electro-fenton oxidation catalyzed by natural pyrite as heterogeneous catalyst. *J. Hazard. Mat.* **2015**, *297*, 34–41. [CrossRef]

159. Ammar, S.; Oturan, M.A.; Labiadh, L.; Guersalli, A.; Abdelhedi, R.; Oturan, N.; Brillas, E. Degradation of tyrosol by a novel electro-Fenton process using pyrite as heterogeneous source of iron catalyst. *Water Res.* **2015**, *74*, 77–87. [CrossRef]

160. El-Desoky, H.S.; Ghoneim, M.M.; Zidan, N.M. Decolorization and degradation of Ponceau S azo-dye in aqueous solutions by the electrochemical advanced Fenton oxidation. *Desalination* **2010**, *264*, 143–150. [CrossRef]

161. Xia, Y.; Shang, H.; Zhang, Q.; Zhou, Y.; Hu, X. Electro generation of hydrogen peroxide using phosphorus-doped carbon nanotubes gas difusion electrodes and its application in electro-Fenton. *J. Electroanal. Chem.* **2019**, *840*, 400–408. [CrossRef]

162. Wang, C.T.; Chou, W.L.; Chung, M.H.; Kuo, Y.M. COD removal from real dyeing wastewater by electro Fenton technology using an activated carbon fiber cathode. *Desalination* **2010**, *253*, 129–134. [CrossRef]

163. Verma, S.K.; Khandegar, V.; Saroha, A.K. Removal of chromium from electroplating industry efuent using electrocoagulation. *J. Hazard. Toxic Radioact Waste* **2013**, *17*, 146–152. [CrossRef]

164. Thor, S.H.; Ho, L.N.; Ong, S.A.; Abidin, C.Z.A.; Heah, C.Y.; Nordin, N.; Yap, K.L. Discovering the roles of electrode distance and confguration in dye degradation and electricity generation in photocatalytic fuel cell integrated electro-Fenton process. *Sep. Purif. Technol.* **2022**, *278*, 119652. [CrossRef]

165. Hu, Y.; Lu, Y.; Liu, G.; Luo, H.; Zhang, R.; Cai, X. Effect of the structure of stacked electro-Fenton reactor on treating nanofiltration concentrate of landfill leachate. *Chemosphere* **2018**, *202*, 191–197. [CrossRef] [PubMed]

166. Suárez-Eiroa, B.; Fernández, E.; Méndez-Martínez, G.; Soto-Oñate, D. Operational principles of circular economy for sustainable development: Linking theory and practice. *J. Clean. Prod.* **2019**, *214*, 952–961. [CrossRef]

167. Gallego-Schmid, A.; Tarpani, R.R.Z. Life cycle assessment of wastewater treatment in developing countries: A review. *Water Res.* **2019**, *153*, 63–79. [CrossRef]

168. Rahimi, S.; Modin, O.; Mijakovic, I. Technologies for biological removal and recovery of nitrogen from wastewater. *Biotechnol. Adv.* **2020**, *43*, 107570. [CrossRef] [PubMed]

169. Mohammed, A.J.; Ismail, Z.Z. Slaughterhouse wastewater biotreatment associated with bioelectricity generation and nitrogen recovery in hybrid system of microbial fuel cell with aerobic and anoxic bioreactors. *Ecol. Eng.* **2018**, *125*, 119–130. [CrossRef]
170. Rotz, C.A. Modeling greenhouse gas emissions from dairy farms. *J. Dairy Sci.* **2018**, *101*, 6675–6690. [CrossRef]
171. Das, A.K.; Saha, C.K.; Alam, M.M. Greenhouse gas emissions from dairy farming in Bangladesh. *World* **2017**, *1*, 092–101. [CrossRef]
172. Gadipelly, C.; Pérez-González, A.; Yadav, G.D.; Ortiz, I.; Ibáñez, R.; Rathod, V.K.; Marathe, K.V. Pharmaceutical industry wastewater: Review of the technologies for water treatment and reuse. *Ind. Eng. Chem. Res.* **2014**, *53*, 11571–11592. [CrossRef]
173. Brooms, T.; Apollo, S.; Otieno, B.; Onyango, M.S.; Kabuba, J.; Ochieng, A. Integrated anaerobic digestion and photodegradation of slaughterhouse wastewater: Energy analysis and degradation of aromatic compounds. *J. Mater. Cycles Waste Manag.* **2020**, *22*, 1227–1236. [CrossRef]
174. Bustillo-Lecompte, C.F.; Mehrvar, M. Slaughterhouse wastewater characteristics, treatment, and management in the meat processing industry: A review on trends and advances. *J. Environ. Manag.* **2015**, *161*, 287–302. [CrossRef]
175. Naderi, K.V.; Bustillo-Lecompte, C.F.; Mehrvar, M.; Abdekhodaie, M.J. Combined UV-C/H_2O_2-VUV processes for the treatment of an actual slaughterhouse wastewater. *J. Environ. Sci. Health B* **2017**, *52*, 314–325. [CrossRef]
176. Yazdani, M.; Ebrahimi-Nik, M.; Heidari, A.; Abbaspour-Fard, M.H. Improvement of biogas production from slaughterhouse wastewater using biosynthesized iron nanoparticles from water treatment sludge. *Renew. Energ.* **2019**, *135*, 496–501. [CrossRef]